# USE OF STANDARD SUMPS FOR SUSPENDED SEDIMENT REMOVAL FROM STORMWATER

**A THESIS**
**SUBMITTED TO THE FACULTY OF THE GRADUATE SCHOOL**
**OF THE UNIVERSITY OF MINNESOTA**

**BY**

**Adam Keith Howard**

**IN PARTIAL FULFILLMENT OF THE REQUIREMENTS**
**FOR THE DEGREE OF**
**MASTER OF SCIENCE**

**Advisors: Heinz Stefan, Omid Mohseni**

**JUNE 2010**

## Acknowledgements

I would like to thank the Minnesota Department of Transportation for providing the funding for this project.

Drs. Heinz Stefan, Omid Mohseni, and John Gulliver spent countless hours patiently guiding me from initial experimental design, to data analysis, to final manuscript. Without their knowledge and expertise this document and the experimental results it contains would not have been possible. They are owed my sincerest thanks and praise.

Benjamin Plante, Patrick Brokamp, Teigan Gulliver, Kurt McIntire, and Andrew Sander assisted with laboratory analysis and construction of the experimental setup. Mike Plante, Andrew Fyten, Matthew Lueker, and Benjamin Erickson from St. Anthony Falls Laboratory provided significant insight for the experimental device setup. Julia Molony and the University of Minnesota's Statistical Clinic provided invaluable help for the uncertainty analysis of the performance functions.

I would also like to thank the Technical Advisory Panel members Barbara Loida, the Technical Liaison (Mn/DOT), Shirlee Sherkow, the Administrative Liaison (Mn/DOT), Jack Frost (Metropolitan Council), Scott Anderson (City of Bloomington), Brett Troyer (Mn/DOT), Beth Neuendorf (Mn/DOT), and Lisa Sayer (Mn/DOT) for their feedback and guidance throughout the project.

# Abstract

There are many standard sumps in urban stormsewer systems that may qualify as a best management practice to pre-treat stormwater runoff by removing suspended sediment from the water. However, no data on the effectiveness of sediment removal and required maintenance schedules of standard sumps exist. Such data could justify providing pollution prevention credits for the use of standard sumps. The goals of this study are to (1) evaluate several standard sump configurations for sediment capture and washout; (2) develop sediment capture and washout functions for the assessment and design of standard sumps as stormwater treatment devices; and (3) design a retrofit for standard sumps to increase sediment capture and decrease washout.

To determine how much suspended sediment they remove from stormwater runoff, two standard sumps of different size and a scale model sump were tested in a laboratory setting. Removal efficiency under low flow conditions as well as sediment washout rate under high flow conditions was measured. The sumps did remove suspended sediment at low flows, but at high flows the washout was substantial.

A porous baffle, named SAFL Baffle, was designed and tested as a possible retrofit to the standard sump. Results indicate that, with the correct baffle configuration, the washout of sediments accumulated in the sump can be nearly eliminated for flows up to approximately the 10-year design storm runoff, and removal efficiency can be increased by 10 to 15%.

A dimensionless scaling parameter was derived for the performance of standard sumps. The scaling parameter incorporates the most influential independent variables. A sediment removal efficiency function and a washout function were developed from the experimental data using the scaling parameter. The functions can serve as a tool for the selection of sumps and the evaluation of other settling devices. The uncertainty in the model predictions has been evaluated by utilizing the bootstrap method. The data collected prove that with a proper maintenance schedule, and/or by the addition of the SAFL Baffle, standard sumps can be successfully used as a pre-treatment device for stormwater.

# Table of Contents

# List of Tables

# List of Figures

## Overview

Standard sumps are designed and built to allow access to a storm sewer system for maintenance and to provide a location for pipe junctions. In addition to these two purposes, the flow patterns in some standard sumps may provide opportunities for the removal of suspended sediments from stormwater runoff. However, data on the effectiveness of sediment removal and maintenance schedule of the sumps does not exist. Such data could justify providing pollution prevention credit for the use of standard sumps for transportation departments, municipalities, counties and other local government agencies. Therefore, the objectives of this study were to (1) evaluate several standard sump configurations for sediment capture and washout; (2) develop sediment capture and washout functions for the assessment and design of standard sumps as stormwater treatment devices; and (3) design a retrofit for standard sumps to increase sediment capture and decrease washout. This thesis is the compilation of two manuscripts, which have been prepared for submission to the Journal of Hydraulic Engineering.

The first manuscript (Chapter 1) addresses the results regarding objectives 1 and 2. To determine whether they remove suspended sediment from stormwater runoff, two full scale standard sumps of different size, and one scale model standard sump were tested in a laboratory setting. The standard sumps were straight flow-through sumps with a slight elevation drop between the inlet and outlet pipes. Each device was constructed of fiberglass and installed on a test stand built in the St. Anthony Falls Laboratory of the University of Minnesota.

Separate tests for removal efficiency and washout were conducted on the standard sumps to determine their effectiveness at removing sediment from stormwater during low flows and retaining the captured sediment during high flows. In the low flow removal efficiency tests, sediments of known size distributions were fed at known rates into the influent pipe of each sump. At the conclusion of each test, the sediments removed by the sump were collected, dried and weighed. In the high flow washout tests, a commercially available sediment was placed inside the sump, and the amount of sediment remaining

after the sump had been flushed by high flows for a period of time was measured. The sumps did remove suspended sediment at low flows, but at high flows the washout was substantial.

It was possible to evaluate the standard sump for five different configurations; two configurations of each full scale sump by varying each sump's depth and one configuration for the scale model. The five configurations provided a detailed data set which was used to evaluate different performance functions. The Péclet number, which was previously used by Wilson et al. (2009), is typically used in a three parameter mathematical function to predict the propensity for sediment capture in stormwater settling devices. The extensive data collected from standard sumps showed that the Péclet number accurately predicts sediment capture in standard sumps, however the Péclet number cannot be used for explaining the removal efficiency of different sump sizes using a single function, i.e. the Péclet number cannot be used as a scaling parameter across different sump sizes or even geometrically similar sumps. In order to predict sediment washout, a new function has been derived for scaling of washout in standard sumps.

In chapter 1 it will be shown that the parameters required for predicting sediment washout in standard sumps can also be used for predicting removal efficiency. The proposed washout and removal efficiency functions perform appropriately for the prediction of washout and sediment removal efficiency in standard sumps with various dimensions. In addition, the bootstrap method has been used to create pointwise confidence intervals for the quantification of the uncertainty in the predictions by the removal efficiency and washout models.

The results presented in chapter 1 became the benchmark for the research conducted to meet the third objective of the study. Chapter 2 describes how a porous baffle, named SAFL Baffle, was designed and tested as a possible retrofit to the standard sump. Multiple configurations with varying percent open area and different angles of attack were first evaluated in a scale model. The optimum configuration obtained from the

scale model study was then constructed at the prototype scale and evaluated for both sediment removal efficiency and sediment washout. Results indicate that with the correct baffle configuration, the washout of sediments accumulated in the sump can be nearly eliminated at very high flow rates, and removal efficiencies can be increased by 10 to 15%. The greatest weakness of the standard sump, sediment washout, is eliminated by the SAFL Baffle retrofit.

The research presented in this thesis has four important implications for stormwater best management practices in urban environments: (1) Standard sumps already in use can remove coarse silt and fine sand particles at low flow rates. However, the standard sump exhibits significant washout at high flow rates. Thus, for the standard sump to be considered a sediment capturing device, frequent maintenance is required. (2) Functions developed from the test data can be used for the prediction of sediment washout and removal efficiency in standard sumps. These functions allow to predict the amount of sediment that will be collected in current stormwater infrastructure and to design future sumps for sediment collection. Municipalities, counties and other local governments may be able to attain stormwater credits for currently installed standard sumps. (3) A non-dimensional parameter has been derived to scale and predict both sediment washout and removal efficiency in standard sumps. It is possible to conduct both washout and removal efficiency tests in a scale model of a stormwater treatment device to predict washout and removal efficiency in the geometrically similar full scale device, thus reducing the cost associated with full scale testing. (4) A porous baffle, named the SAFL Baffle, was designed to nearly eliminate the washout potential in standard sumps. The SAFL Baffle can be installed as an inexpensive retrofit in standard sumps to reduce the potential cost of sediment removal from stormwater runoff.

# Chapter 1. Evaluation of Standard Sumps

The standard sump (manhole) has been a key component of urban stormwater management infrastructure. Sumps are placed at pipe junctions and provide access for storm sewer maintenance. The alignment, larger size and flow patterns in a sump provide opportunities for removal of particulate matter. The standard sump is a cylindrical tank with a vertical axis. Sump depths are usually greater than their diameter. The inlet and outlet pipes are typically oriented straight across from each other, with a slight drop from inlet to outlet. However, it is not uncommon for a sump to have more than one inlet or outlet at various locations in the sump. Standard sumps may provide unintentional pre-treatment by removing and retaining sediment from the flowing water, thereby causing sediment removal to be the greatest cost in non-routine maintenance activities (Kang et al 2008).

In recent decades, 'proprietary' devices for the treatment of stormwater have become increasingly popular to aid communities in meeting stormwater quality regulations. These regulations are a response to the 1987 amendments to the Clean Water Act (Smith 2001). While proprietary devices have proven effective as pre-treatment devices that remove inorganic particles larger than silt, their cost has led local governments to explore other avenues to reach their stormwater pre-treatment goals. Many studies have been conducted to evaluate the performance of proprietary devices for stormwater treatment (Carlson et al. 2006, Mohseni et al. 2007, Wilson et al. 2009, Kim et al. 2007).

By comparison, data on the effectiveness of standard sumps are very limited. There are several reports on catch basins which are hydraulically similar to standard sumps (Butler et al. 1995, Avila and Pitt 2008, and Pitt 1985). This literature indicates that catch basin sumps perform poorly for the capture and retention of fine particulates under most flow conditions. Catch basin studies can provide a basic understanding of sediment deposition and washout processes in settling devices. However, actual catch basin removal efficiency and washout values should not be compared to standard sumps due to differences in flow patterns. Faram and Harwood (2003) provide a means of comparing

different settling devices by numerical modeling of catch basins, standard sumps, and simple and complex hydrodynamic separators. They noted that standard sumps perform slightly better than catch basins for removal efficiency and washout.

It is common practice to use sampling at the inflow and the outflow of the sump to evaluate the performance of stormwater best management practices (BMPs). Unfortunately, the use of samplers for monitoring of influent and effluent has proven unreliable for the collection of particles larger than medium silt (Wilson et al. 2007, DeGroot et al. 2009). However, Wilson et al. (2009) assessed the removal efficiency of four hydrodynamic separators in the field by utilizing a mass balance approach. Three discrete particle sizes in the ranges 89-125μm, 251-355μm, and 500-589μm were released by a calibrated sediment feeder into the water upstream of each separator device. At the conclusion of a test the separator device was carefully cleaned and all sediment which was deposited was collected, dried, sieved and weighed. This same mass balance approach was also used by Carlson et al. (2006) and Mohseni et al. (2007) for laboratory evaluations of two other stormwater settling devices.

Mohseni et al. (2007) evaluated the washout potential for a hydrodynamic separator. A mass balance approach was also chosen for this study. The separator was preloaded with sediment, and the preloaded sediment depth was measured at many locations to estimate the pre-test sediment volume. Following a high flow test, the remaining sediment depth and volume was measured, and the difference provided a value for the sediment washout. This procedure was also followed by Saddoris et al. (2010) for the evaluation of the sediment washout from other hydrodynamic separators. Three hydrodynamic separators where tested in the laboratory, and one was tested in the field. In the field sediment depth was measured using a hand ruler and/or laser levels. In the laboratory the separator devices were set on strain gauge load cells, to provide continuous, accurate monitoring of the sediment weight.

The goals of this study were to (1) evaluate four configurations of a straight flow-though standard sump for sediment capture and washout; (2) develop a performance function for

the removal of suspended sediments from a standard sumps; (3) develop another performance function for the sediment washout from a standard sump; (4) conduct an analysis of the uncertainties in the performance functions.

Terminology for the description of sediment capture and washout of stormwater BMP devices varies from one study to another. Often, the terms 'treatment', 'performance', or 'removal efficiency' are used to describe the overall ability of a device to remove sediment from the influent and deposit it at the bottom of the sump. The terms treatment and performance can be confused because it is not clear whether the net effect of the entire sediment capture, retention and release processes in the device is described, or whether the terms refer to deposition and retention (deposition minus washout) separately. Herein, the term "removal efficiency" is applied to describe the efficiency of the deposition process only. The terms 'retention', 'scour', 're-suspension', or 'washout' are often used to describe the ability of a settling device to retain the previously captured sediment. However, it is possible for scour and re-suspension to occur in a settling device without the sediment actually leaving the device. The term retention also has connotations regarding the capture of sediment. Herein, the term 'washout' is used to describe the amount of previously captured sediments that are scoured, resuspended and washed out (carried away) from the device.

## 1.1 Experimental Setup and Procedures

### 1.1.1 Experimental Setup

Two full scale fiberglass sumps were placed on a test stand in the St. Anthony Falls Laboratory (SAFL) of the University of Minnesota in Minneapolis, Minnesota. The first sump evaluated was 1.2m (4ft) in diameter with a 1.2m (4ft) height from the invert of the inlet pipe to the sump bed, with 0.38m (15in) inlet and outlet pipes at 0 and 180 degrees, respectively. To evaluate the performance of a shallow 1.2m (4ft) sump, a false floor was placed in the sump to decrease the sump depth to 0.6m (2ft). There was a one percent drop between the inlet and outlet pipes.

The second sump was 1.8m (6ft) in diameter and 1.8m (6ft) high with 0.6m (24in) inlet and outlet pipes at 0 and 180 degrees, respectively. A false floor was also added to this configuration to create a 1.8m (6ft) diameter with a 0.9m (3ft) height. Each sump was connected to the SAFL plumbing system which provided approximately 13.7m (45ft) of head of Mississippi River water. Discharge was measured using a pitot cylinder (Silberman, 1947) upstream of the device. In both configurations, discharge was controlled using hydraulic gate valves on the supply pipes. Figures 1.1 and 1.2 are drawings of the 1.2m (4ft) and 1.8m (6ft) diameter sumps, respectively.

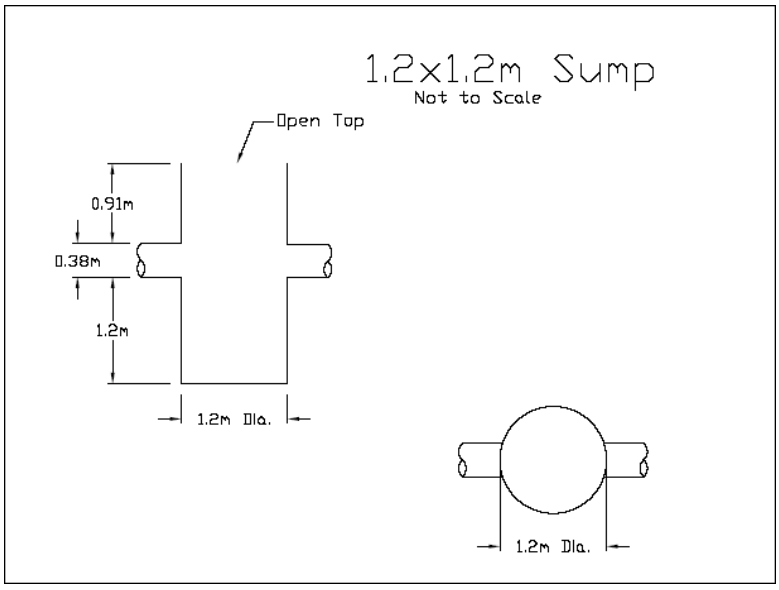


**Figure 1.1: 1.2m (4ft) diameter standard sump drawing showing both plan and profile views**

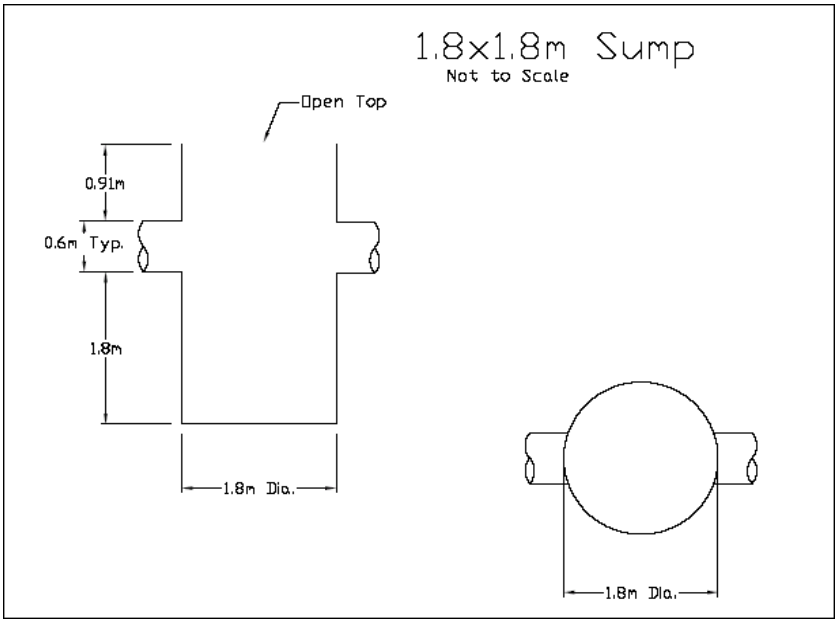


**Figure 1.2: 1.8m (6ft) diameter standard sump drawing showing both plan and profile views**

In addition to the full size models tested in the laboratory, a scale model of the 4×4 (1.2m (4ft) in diameter and 1.2m (4ft) in height) sump was built for testing. The scale model was constructed of clear acrylic plastic at the scale of 1:4.17. Tap water was re-circulated using an electric pump and two head tanks. The effluent from the model would pass through a 20 μm filter, and then would re-enter one of the head tanks.

### 1.1.2 Testing Procedures

To avoid the problems associated with suspended sediment sampling, the mass balance approach employed by Carlson et al. (2006), Mohseni et al. (2007), Wilson et al. (2009), and Saddoris et al. (2010) was adopted in this study to assess the sediment removal efficiency and sediment washout. For performance testing, sediment was fed as slurry from a Schenk AccuRate sediment feeder into the inlet pipe one foot upstream of the sump. A manometer rack was connected to the device for recording water surface elevations in the inlet pipe, the sump, and the outlet pipe. For testing of sediment washout, the sump was mounted on precision strain gauge load cells. The load cells allowed for accurate measurement of weight before, during, and after tests. For the model, sediment caught on the filter was used to determine washout, and sediment that was captured in the sump model was used to determine retention efficiency.

For the 1.2m (4ft) sump removal efficiency testing, discharges were set at 17L/s, 34L/s, 51L/s, and 68L/s (0.6, 1.2, 1.8, 2.4cfs) and each test was repeated three times. The 1.8m (6ft) sump was tested at discharges of 51L/s, 99 L/s, 150L/s, and 200 L/s (1.8, 3.5, 5.3, 7cfs) in triplicate. Three distinct particle sizes were used for the tests. The three median sediment sizes were, 545μm (500μm to 58μm), 30 μm (25μm to 355μm), and 107μm (88μm to 125μm). The sieve sizes where chosen so one sieve size remained between each particle size to allow no overlap of particles and to minimize the errors associated with particle sizes (Wilson et al. 2007).

Sediment washout tests involved preloading the sump with sediment and then applying high discharges through the sump. Twelve inches of the F-110 Silica sand with a median particle size of 110μm was placed in the sump. Two methods were used to measure the sediment washout rate: (1) a volume-based method and (2) a weight-based method. In the volume-based method, stick measurements were taken to find the depth of sediment at 24 locations, which was then used to approximate the average depth of deposit. This average depth was then used to estimate the weight of the sediment with the knowledge of the sump bed area and the average bulk density of wet sediment. To determine the in situ bulk density, a testing protocol was created which involved measuring the bulk density of multiple samples which were obtained before and after each test. The development of the protocol involved the creation of sediment packing and leveling techniques which provided repeatable results for both the sediment in the sump and the sediment samples.

The weight-based measurement of sediment washout involved the use of precision strain gauge load cells. Three 2268kg (5000lb) rated load cells were placed under a steel frame for which the 1.2m (4ft) diameter sump rested on. The 1.8m (6ft) diameter sump rested on 4 load cells. Water level readings were taken both before and after the tests using a monometer which was accurate to 0.3mm (0.001ft). The difference in water levels, and subsequent weight difference, could then be accounted for. In addition, the inlet and outlet pipes, as well as any other monometer or drain connections for the sump, were disconnected while the readings were being taken to ensure no outside weight influences would affect the accuracy. The load cells provided a precise measure of the change of

weight throughout the test. The discharge rates for the 1.2m (4ft) sump varied from 78 L/s to 160L/s (2.75 to 5.5cfs). The discharges for the 1.8m (6ft) sump varied from 140L/s to 540 L/s (5 to 19cfs).

## 1.2 Results

### 1.2.1 Removal Efficiency and Washout

Data of all measured removal efficiencies of the standard sumps tested are plotted versus discharge in Figure 1.3. The figure illustrates trends for the capture of sediment in 1.8×1.8m (6×6ft), 1.8×0.9m (6×3 ft), (1.2×1.2m) 4×4ft, 1.2×0.6m (4×2ft), and 0.3×0.3m (1×1ft) sumps for three different particle sizes (110µm, 335µm, 545µm). As discharge decreases or particle size increases, removal efficiency of the standard sump increases, as would be expected. Also, for the same particle size and discharge, as the depth and diameter of the sump increases, the removal efficiency of the sump increases. In other words, a 1.8×1.8m (6×6ft) sump will perform better than a 1.2×1.2m (4×4ft) sump, and a 1.8×0.9m (6×3ft) sump will perform better than a 1.2×0.6m (4×2ft) sump.

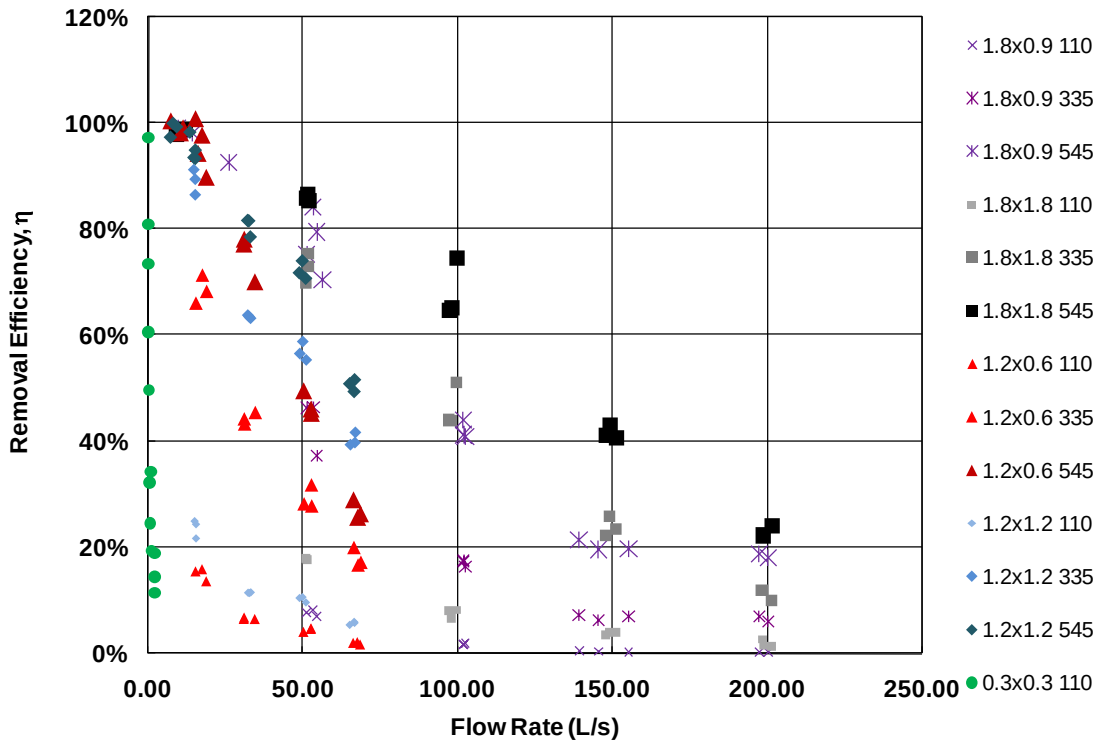


**Figure 1.3: Sediment deposition (removal efficiency) results obtained at low discharges. Legend gives sump size (diameter x depth in m), and particle size in µm**

Sediment washout in terms of effluent concentration versus discharge is shown in Figure 1.4. All of the washout data were collected for the same particle size (110μm). Figure 1.4 shows that as the discharge increases the effluent concentration increases until the discharge becomes sufficiently high for the inflow jet to begin short-circuiting. Once short circuiting occurs the effluent concentration slightly decreases. For the same discharge the 1.8×1.8m (6×6ft) sump can be expected to retain the captured sediment better than the 1.8×0.9m (6×3ft) sump. Similarly, the 1.2×1.2m (4×4ft) sump retains the sediment better than the 1.2×0.6m (4×2ft) sump. In addition, the 1.8×0.9m (6×3ft) sump retains the sediment better than the 1.2×1.2m (4×4ft) sump.

The results of the washout tests revealed a noticeable decrease in effluent concentration when the discharge became very high. This was attributed to short circuiting of the discharge through the sump.

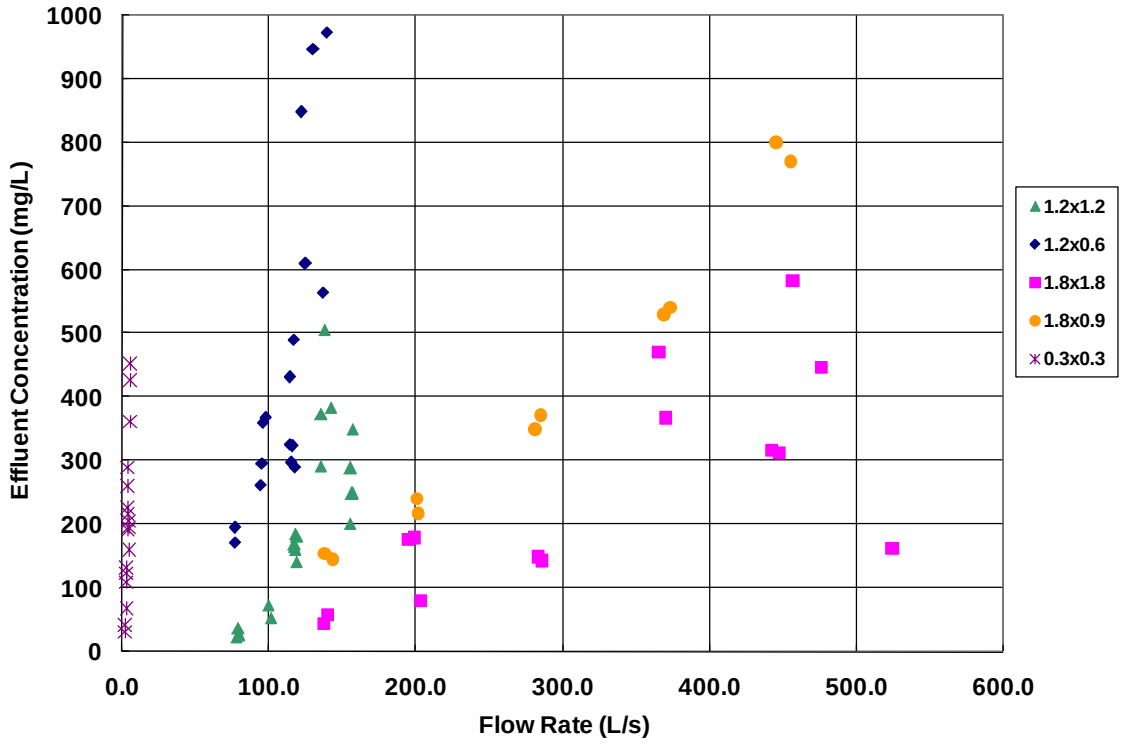


**Figure 1.4: Sediment washout results obtained at high discharges. Legend gives sump size (diameter x depth in m)**

### 1.2.2 Velocity Measurements

In order to understand and explain the processes involved in washout and deposition within the sump, flow mapping experiments were conducted using a 3-Dimensional Acoustic Doppler Velocimeter (ADV). Figure 1.5 gives a velocity vector plot that illustrates the circulation pattern in a standard sump. Water entering the sump as a horizontal jet spreads downwards, causing plunging and a downward velocity at the downstream end of the sump, and upward velocity at the upstream end. The surface of the sediment bed becomes sloped due to the scour at the downstream side of the deposit and deposition at the upstream side of the sump. Figure 1.6 gives an overhead photo and a side view sketch of the sediment deposit at the bottom of the sump following a high flow washout test.

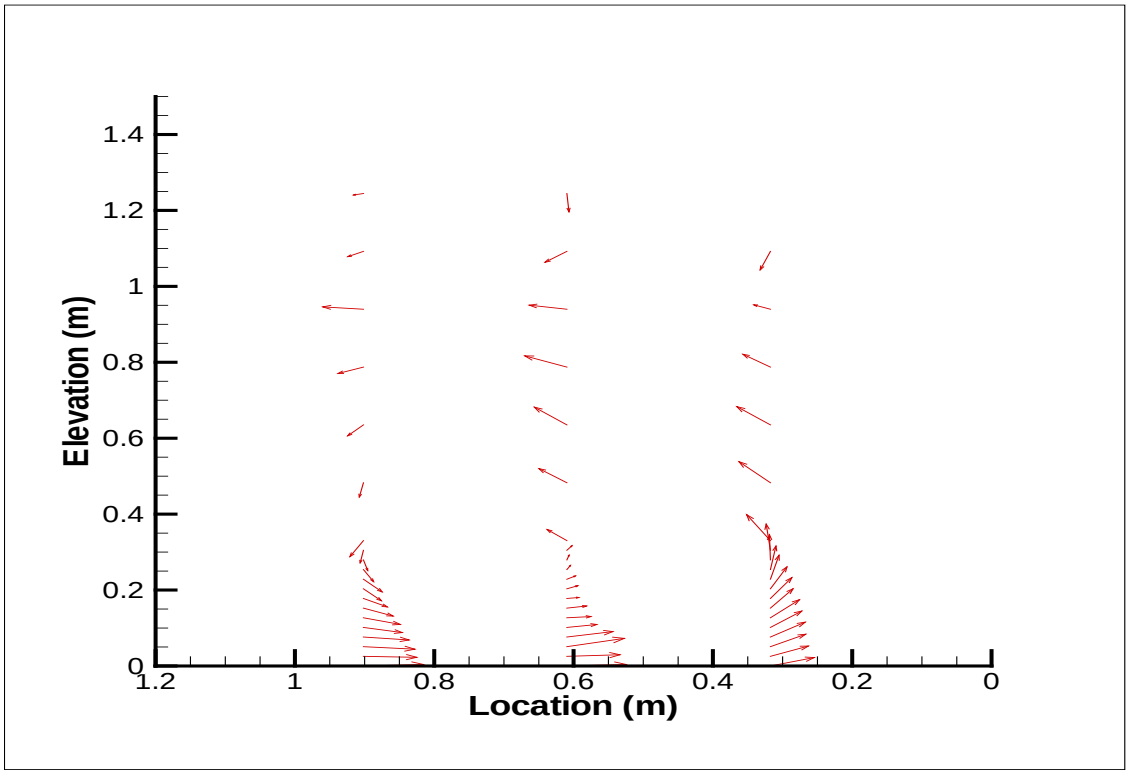


**Figure 1.5: Velocity vectors in the vertical center plane of a deep sump. Inflow velocity is 0.85m/s (2.8 ft/s) from right to left, invert of inflow pipe is at 1.2m (48in) elevation.**

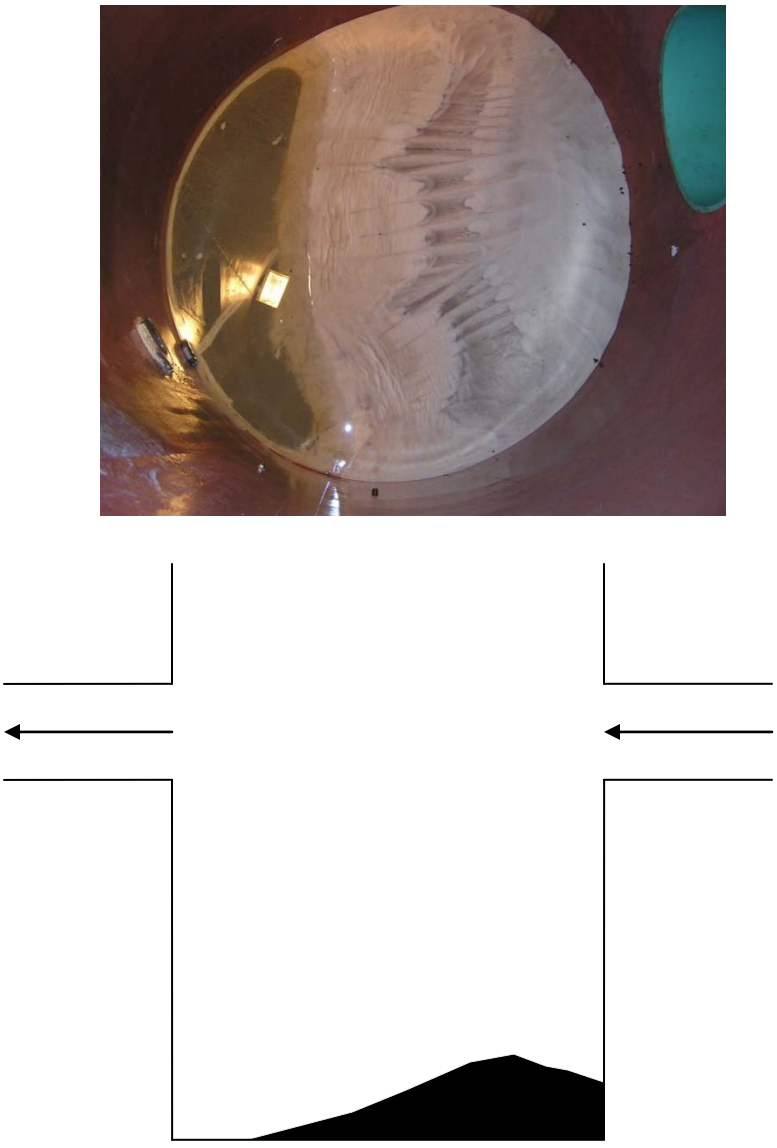

**Figure 1.6: Overhead view and side view of the sediment deposits at the bottom of the sump after a washout test. Flow in the test was from right to left. Clear dark area on the left of the overhead photo is the sump bottom without sediment deposits.**

Short-circuiting of the flow through a standard sump at high discharges was verified by vertical velocity profiles in the sump. Figure 1.7 gives the vertical component $V_z$ of flow

velocity in the sump versus height above the sump bottom at a location 16 inches upstream of the outlet pipe. Because the discharge through the sump was varied from 130 to 170L/s (4.5 to 6.0cfs), the velocity components $V_z$ are normalized by the inflow velocity $V_{jet}$. At the lower discharges, the flow direction was downward (negative velocity) over the entire water column in the sump. At the higher discharges, the flow direction was upward (positive velocity) over 20% of the crown height in the sump. Thus, the flow through the sump was no longer plunging into the sump at higher discharges, but short-circuiting to the outlet, thus decreasing the energy available for sediment suspension at the bottom of the sump, and washout. However, a vortex with horizontal axis still existed in the lower 80% of the sump depth, i.e. the circulation pattern above the sediment deposit did not disappear completely, but as is evident in Figure 1.7, its strength dropped and the washout rate decreased.

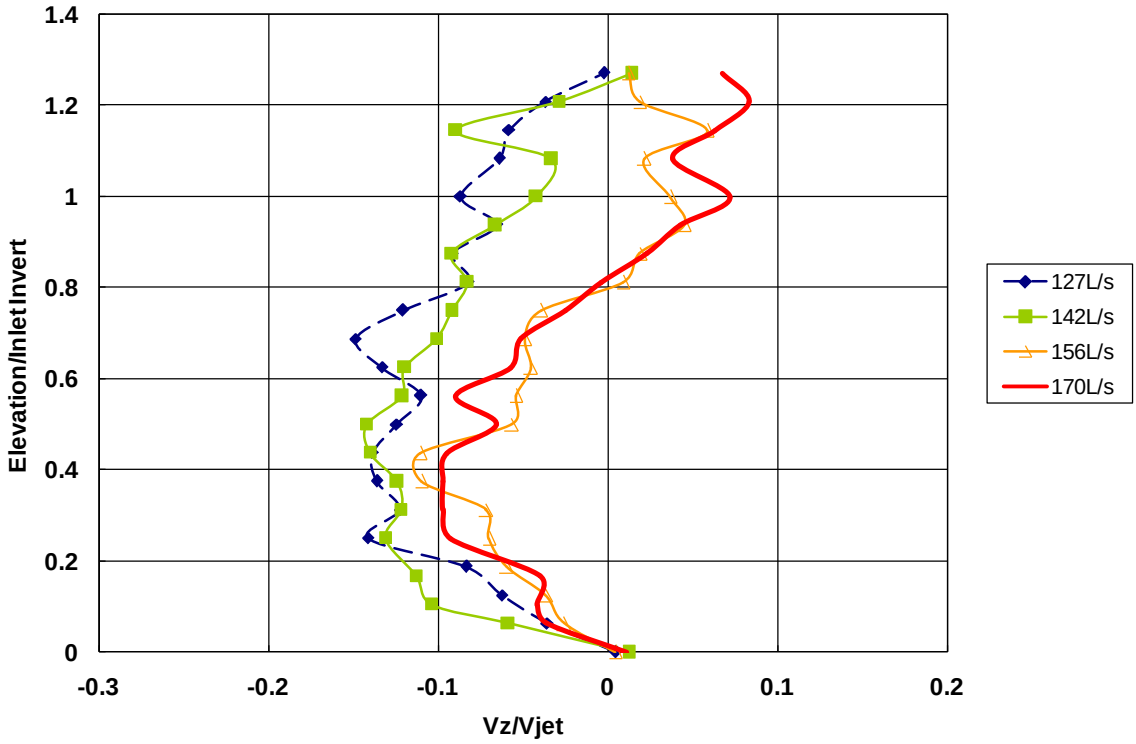


**Figure 1.7: Normalized vertical velocity vs. depth. Measurements taken 0.4m (16in) upstream of outlet.**

## 1.3 Scaling

### 1.3.1 Removal Efficiency/Péclet Number

To define the performance (removal efficiency) of a proprietary device for the entire range of discharges, particle sizes, densities, and viscosities, without testing all flow conditions and particles, Wilson et al. (2009) used a Péclet number. This Péclet number is based on previous analyses by Dhamotharan et al, (1981) and is the ratio of convective transport by settling to turbulent diffusion. The convective, settling process of particles is opposed by turbulent diffusion tending to keep sediment in suspension. The Péclet number, so defined, is directly proportional to the particle settling velocity ($U_s$), sump diameter ($D$) and sump depth (h), and is inversely proportional to the discharge ($Q$) through the sump, thus

$$Pe = \frac{U_s hD}{Q} \tag{1.1}$$

The settling velocity ($U_s$) in Equation 1.1 can be determined in a variety of ways. We shall calculate it using the equation developed by Cheng (1997). When the measured removal efficiencies *($\eta$)* are plotted versus Péclet numbers *(Pe)* obtained for each test, a function *$\eta$(Pe)* can be fitted to the data to explain the overall removal efficiency of the sump, i.e. a performance function *$\eta$(Pe)* can be developed. This procedure involving the Péclet number works well for the prediction of removal efficiency of an individual device. Sumps of different sizes may require different fitted functions. An example is presented in Figure 1.8, where the fitted function of a 1.2x1.2m (4×4ft) sump is different from a 1.2×0.6m (4×2ft) sump.

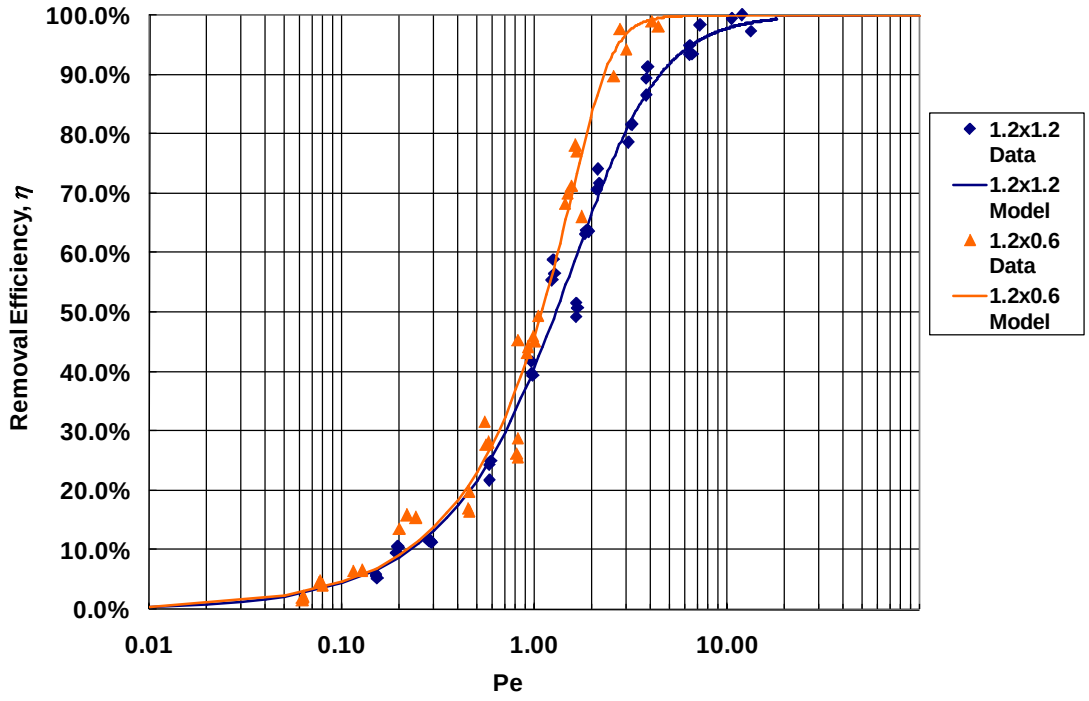


**Figure 1.8: Performance functions of 1.2×1.2m (4×4ft) and 1.2×0.6m (4×2ft) standard sumps. Legend provides sump dimensions (diameter x depth) in m.**

### 1.3.2 Sediment Washout Process

As observed by Saddoris et al. (2010), washout from a stormwater treatment device under high flow conditions is comprised of the following: (1) setting in motion of particles on the surface of the sediment deposit, (2) entrainment of particles into the water column in the sump above the sediment deposit, and (3) lifting of particles up to the effluent pipe and out the effluent pipe. The energy (power) supplied by the water flowing into the sump should exceed the work (power) required for the above three processes.

To quantify washout in stormwater treatment devices, the energy supplied by the inflow, and the required work for the above processes were further studied. In order to compare the supplied energy with the required work, these scalars were estimated per unit of time, i.e. in terms of power.

The power supplied by the inflow to the sump is

$$P_{\sup} = \rho_w Q \frac{U_j^{\,2}}{2} \tag{1.2}$$

where $\rho_w$ is the water density, $Q$ is discharge , and $U_j$ is the inlet jet velocity.

The energy associated with the head loss through the sump is the amount of energy to overcome the head loss at the inlet, at the exit, due to wall friction in the sump and work required for sediment washout. Only a fraction of the power associated with the lead loss is used to cause washout in the sump. The power associated with the head loss can be estimated as

$$P_{loss} = gQh_L\rho_w \tag{1.3}$$

In Equation 1.3, $h_L$ is the head loss through the sump, which can be estimated using the energy equation between the inlet and outlet of the sump.

$$h_L = h_{in} + \frac{U_{in}^{\,2}}{2g} - \left( h_{out} + \frac{U_{out}^{\,2}}{2g} \right) \tag{1.4}$$

In Equation 1.4, $h_{in}$ and $h_{out}$ are the water surface elevations from a common datum in the inlet and outlet pipes (or gage pressures) of the sump, respectively, and $U_{in}$ and $U_{out}$ are the inflow and outflow velocities, respectively. The power lost (Equation 1.3) will include both the power which provided work on the sediment, and the power which is lost as heat due to turbulence. In other words, the power used in sediment washout will be the total power lost minus the power lost to heat. The power lost to heat will include the wall friction and entrance and exit losses. Thus the power available for sediment washout is

$$P_{sed} = P_{loss} - \left( P_f + P_{entrance} + P_{exit} \right). \tag{1.5}$$

In Equation 1.5, $P_{sed}$ is the power used for washout, and $P_f$, $P_{entrance}$, and $P_{exit}$ are the power losses associated with friction loss, entrance loss and exit loss, respectively. By measuring discharge and water depths at the inlet and outlet, the total power supplied and the total power lost to the sump due to heat and sediment washout can be quantified. Unfortunately, quantifying the power loss due to heat in a sump is subject to substantial

uncertainties. Subsequently, quantifying the actual power available for sediment washout is also uncertain.

As stated earlier, sediment washout begins with incipient motion of the bed particles. The power required to initiate the motion of the particles can be approximated by

$$P_{sc} = \tau_c A U \tag{1.6}$$

In Equation 1.6, $\tau_c$ is the critical shear stress for the incipient motion of particles, $A$ is the surface of the deposit and $U$ is the average velocity of particles. This velocity can be approximated by the critical shear velocity $U_{*sc}$ as given in Equation 1.7.

$$U_{*sc} = \sqrt{\frac{\tau_c}{\rho_w}} \tag{1.7}$$

Replacing the critical shear stress with $\rho_w U_{*sc}^2$, Equation 1.6 can be rearranged as follows.

$$P_{sc} = \rho_w U_{*sc}^3 A \tag{1.8}$$

Using the Shields diagram, one can estimate the critical shear stress $\tau_c$ for the movement of a particular sediment size with a given density (Vanoni 1975). The associated critical shear velocity $U_{*sc}$ can then be estimated and placed in Equation 1.8 to estimate the power necessary for bed load movement.

If there is still energy available following the bed load movement, it will be utilized for the particle entrainment into the water column. The particle entrainment can be parameterized by

$$P_{ent} = \rho_w U_{*ent}^3 A. \tag{1.9}$$

In Equation 1.9, $U_{*ent}$ is the critical shear velocity for entrainment which can be estimated using the results of the research conducted by Akiyama and Stefan (1985) on turbidity currents. This critical shear velocity occurs when the suspended sediment concentration is near zero. Akiyama and Stefan (1985) defined the suspended sediment concentration by a

dimensionless parameter, $E_s$, which is the sediment entrainment. Sediment entrainment approaches zero at a value of approximately

$$\frac{U_{*ent}}{U_s} R_p^{0.5} = 6. \tag{1.10}$$

In Equation 1.10, $U_s$ is the particle settling velocity and $R_p$ is the particle Reynolds number.

$$R_p = \frac{d\sqrt{SGgd}}{\nu}. \tag{1.11}$$

In Equation 1.11, *SG* is the specific gravity of the sediment, *d* is the particle diameter, and $\nu$ is the kinematic viscosity of the fluid (water). Inserting Equation 1.11 into Equation 1.10 and solving for $U_{*ent}$ results in Equation 1.12:

$$U_{*ent} = \frac{6U_s \nu^{0.5}}{d^{0.5}(SGgd)^{0.25}} \tag{1.12}$$

The results of Equation 1.12 can then be used to estimate the power required for particle entrainment in Equation 1.9.

Once the sediment has become entrained, additional power is required to hold the sediment in suspension. If the remaining supplied power exceeds this power and is large enough to lift the suspended particles in the water column up to the outlet pipe, the power $P_{set}$ necessary to overcome settling of the particles concentration $\overline{C}$ is

$$P_{set} = \frac{\overline{C}aAg(SG-1)U_s}{SG}, \tag{1.13}$$

where $\overline{C}$ is the average sediment concentration, *a* is the sump's water column, and *A* is the sump cross-sectional area. The average concentration of sediment in the sump is not known unless it is sampled. If washout occurs in a sump then the parameter *a* can be set equal to *h*, the height of the outlet invert from the deposit surface. In order to determine if a well-mixed condition can exist in a standard sump, such that $\overline{C} = C$, the one-

dimensional advection-diffusion equation under steady state condition (Equation 1.14) was analyzed for the sump.

$$-U_s \frac{\partial C}{\partial z} = \frac{\partial}{\partial z}\left(\left(\overline{\varepsilon_z}\right)\frac{\partial C}{\partial z}\right) \tag{1.14}$$

$C(z)$ in Equation 1.14 is the concentration at a given depth $z$ above the sediment bed, $\overline{\varepsilon_z}$ is the mean turbulent diffusion coefficient, assuming a mean turbulent diffusion is sufficient to explain the entire diffusion process in the sump. Equation 1.14 after integration becomes

$$C = \beta\, e^{-U_s z/\overline{\varepsilon_z}}, \tag{1.15}$$

In Equation 1.15, $\beta$ is the constant of integration. It is possible to compare the concentration near the top, i.e. near the invert of the outlet pipe, and at the sediment bottom of the sump as the ratio of the two concentrations:

$$\frac{C_{top}}{C_{bottom}} = e^{-U_s h/\overline{\varepsilon_z}}. \tag{1.16}$$

In Equation 1.16, $h$ is the elevation at the top of the sump; the elevation at the bottom of the sump (sediment surface) was set equal to zero. The equation proposed by Prandtl (Schetz 1993) can be used for approximating the average turbulent diffusion coefficient.

$$\overline{\varepsilon_z} = \kappa\, \Delta U_x\, f\, h \tag{1.17}$$

In Equation 1.17, κ is the von Karman constant, $\Delta U_x$ is the change in velocity across the height of the eddy, and $f$ is the fraction of the total water depth $h$ in the sump which contains the large eddy. By incorporating Equation 1.17 into Equation 1.16, one obtains

$$\frac{C_{z=h}}{C_{bottom}} = e^{\frac{-U_s h}{k\Delta U_x f h}} = e^{\frac{-U_s}{k\Delta U_x f}}. \tag{1.18}$$

Using the velocity measurements taken at the horizontal center of the 1.2×1.2m sump (Figure 1.9), the $\Delta U_x$ and $f$ are estimated to be about 1.05m/s and 0.72, respectively.

These values are relatively typical values in standard sumps under high discharge conditions. For a particle size with a $d_{50}$ = 110μm, the settling velocity at 20°C (68°F) becomes 0.0046m/s (0.015ft/s). Using a value κ = 0.4 and quantifying the right-hand side of Equation 18 using the above estimates, the left-hand side of Equation 1.18 becomes 0.985, indicating that the suspended sediment in the 1.2×1.2m sump is close to well-mixed at these discharges.

The concentration at the sump outlet drops to 90% of the near bed concentration only when the particle size exceeds 340μm. Therefore, a well mixed condition in the sump under high flow conditions is a realistic assumption.

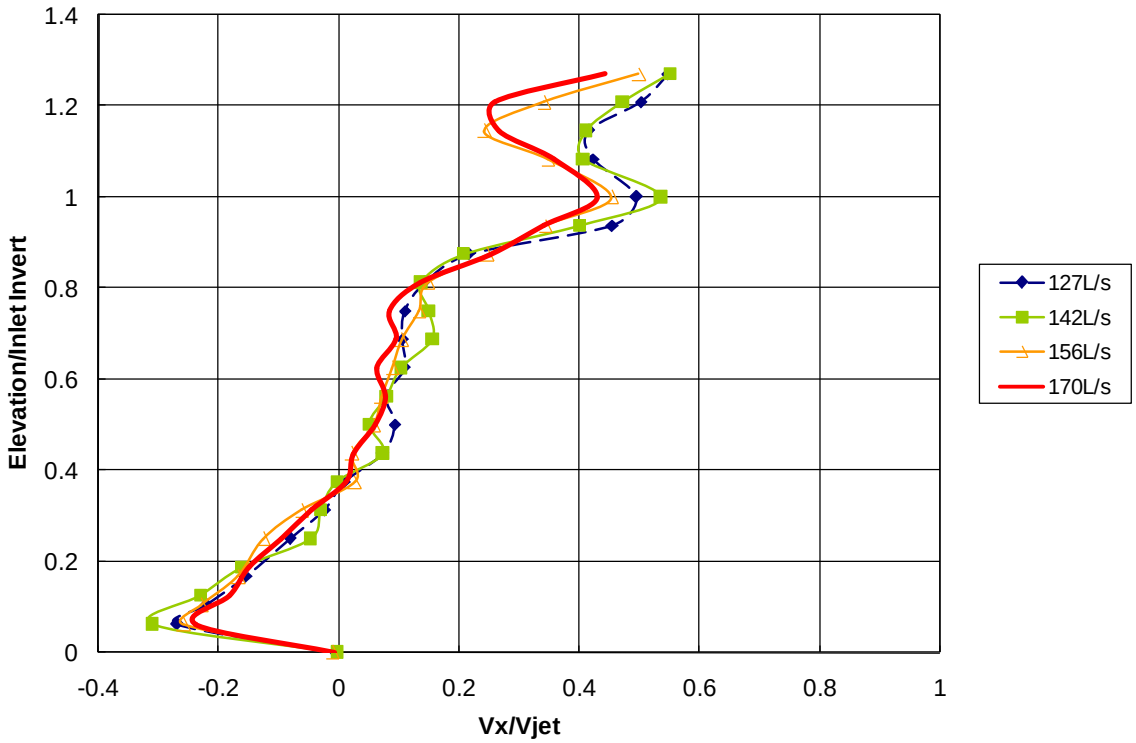


**Figure 1.9: Horizontal velocity vs. depth at the center of a 1.2m (4ft) standard sump.**

If there is enough power available to begin sediment bed motion, to entrain sediment particles into the water column, and to overcome the settling of the resuspended sediments, washout becomes inevitable. To examine this, the powers parameterized in Equations 1.2, 1.3, 1.8, 1.9 and 1.12 have been quantified and tabulated in Table 1.1 for

all tested discharges. The power supplied to the sump is in all cases significantly greater than any of the powers necessary for scour, entrainment, or to overcome settling. The power loss in the sump is about three orders of magnitude larger than the sum of these three powers. This indicates that more than 99% of the power loss is due to the entrance, exit and frictional losses in the sump.

When the power loss in the sump is about 10 to 15% of the power supplied by the inflow, the experimental data shows that washout concentration is very small, i.e. about 30mg/L (Table 1.1), which is within the measurement error of the experiments. As the power loss becomes a larger fraction of the supplied power, i.e. 20% and more, washout increases significantly. When the power loss exceeds 70% of the supplied power, the effluent concentration reaches 400 to 500mg/L.

The values tabulated in Table 1.1 clearly show that with very little power the sediment deposit can be disturbed and even entrained into the water column. Therefore, bed forms may easily develop in standard sumps but washout may never happen. This process was also observed by Saddoris et al (2010) for hydrodynamic separators.

Table 1.1 also indicates that head loss drops at the highest discharges of 160L/s (5.5cfs), which is another indicator of the short-circuiting described previously.

**Table 1.1: Data on powers in sediment washout experiments with a 4×4ft sump.**

| Flow Rate (L/s) | Supplied Power $P_{sup}$ (Nm/s) | Head Loss $h_L$ (m) | Power Loss (Nm/s) | Power for Scour (Nm/s) | Power for Entrain. (Nm/s) | Power for Settling $P_{set}$ (Nm/s) | $P_{set}/P_{sup}$ | Eff. Conc (mg/L) |
|---|---|---|---|---|---|---|---|---|
| 79 | 1.9 | 0.01 | 0.2 | 0.00016 | 0.00013 | 0.00003 | 0.000018 | 27 |
| 79 | 1.8 | 0.00 | 0.1 | 0.00016 | 0.00013 | 0.00005 | 0.000026 | 37 |
| 77 | 1.7 | 0.01 | 0.3 | 0.00016 | 0.00013 | 0.00003 | 0.000018 | 24 |
| 117 | 3.6 | 0.02 | 1.0 | 0.00016 | 0.00013 | 0.00021 | 0.000059 | 161 |
| 119 | 3.8 | 0.02 | 1.1 | 0.00016 | 0.00013 | 0.00024 | 0.000064 | 181 |
| 118 | 3.7 | 0.02 | 1.0 | 0.00016 | 0.00013 | 0.00019 | 0.00005 | 141 |
| 117 | 3.6 | 0.02 | 0.9 | 0.00016 | 0.00013 | 0.00023 | 0.000064 | 169 |
| 117 | 3.6 | 0.02 | 1.1 | 0.00016 | 0.00014 | 0.00026 | 0.000071 | 186 |
| 117 | 3.8 | 0.01 | 0.8 | 0.00016 | 0.00014 | 0.00023 | 0.000061 | 165 |
| 99 | 2.6 | 0.01 | 0.5 | 0.00016 | 0.00023 | 0.00015 | 0.000056 | 73 |
| 101 | 2.8 | 0.01 | 0.4 | 0.00016 | 0.00023 | 0.00011 | 0.000038 | 54 |
| 142 | 5.2 | 0.05 | 3.4 | 0.00016 | 0.00023 | 0.00083 | 0.00016 | 384 |
| 138 | 4.7 | 0.05 | 3.7 | 0.00016 | 0.00023 | 0.00104 | 0.000221 | 506 |
| 135 | 4.5 | 0.06 | 3.8 | 0.00016 | 0.00023 | 0.00076 | 0.000169 | 373 |
| 135 | 4.5 | 0.05 | 3.6 | 0.00016 | 0.00024 | 0.00060 | 0.000134 | 291 |
| 156 | 6.9 | 0.03 | 2.0 | 0.00016 | 0.00014 | 0.00037 | 0.000053 | 249 |
| 155 | 6.7 | 0.02 | 1.7 | 0.00016 | 0.00014 | 0.00029 | 0.000044 | 202 |
| 156 | 6.9 | 0.02 | 1.8 | 0.00016 | 0.00014 | 0.00037 | 0.000053 | 249 |
| 157 | 7.0 | 0.03 | 2.6 | 0.00016 | 0.00023 | 0.00071 | 0.000102 | 350 |
| 155 | 6.8 | 0.04 | 2.7 | 0.00016 | 0.00023 | 0.00058 | 0.000086 | 289 |

As shown, washout is a function of power supplied and the power required to overcome the incipient motion of particles, particle entrainment into the water column and the power for lifting the particles. In Table 1.1, the power required for scour is constant for the F110 Silica Sand with a median size of 110 microns. The power for entrainment varies by no more than 80%, as effluent concentration increases 30 fold. The only power which increases about the same as effluent concentration is the power required to overcome settling, which can become an order of magnitude larger than the power required for scour. This is natural, because the high concentrations required for substantial washout will also require a greater power to overcome particle settling. It appears that the ratio of power to overcome particle settling to the power supplied can be a good indicator of the washout rate.

### 1.3.3 Washout Function

To develop a washout function, a dimensional analysis was carried out for standard sumps. Ignoring the power required for scour and entrainment, it was determined that the effluent concentration ($C$) during the washout is a function of gravity ($g$), water density ($\rho_w$), particle density ($\rho_s$), sump dimensions ($h$ and $D$), settling velocity of particles ($U_s$), the influent jet velocity ($U_j$), and the discharge ($Q$), i.e.

$$C = f\left(g, \rho_w, \rho_s, h, D, U_s, U_j, Q\right) \tag{1.19}$$

By converting Equation 1.20 to a number of dimensionless parameters one obtains

$$\frac{C}{\rho_w} = \Phi\left(SG, Fr_j, Pe\right) \tag{1.20}$$

In Equation 1.20, $SG$ is the specific gravity of particles, $Fr_j$ is the Froude number of the influent jet velocity defined as

$$Fr_j^{\,2} = \frac{U_j^{\,2}}{gD} \tag{1.21}$$

and $Pe$ is the Péclet number given by Equation 1.1. It is important to note that in the dimensional analysis, one can use the Hazen number (Wilson et al., 2009) instead of the Péclet number.

Before plotting the experimental data obtained in the testing program against these dimensionless numbers, it was determined that the dimensionless parameters in Equation 1.20 can also be obtained from a ratio of the power required to overcome particle settling ($P_{set}$) to the supplied power supplied by the inflow ($P_{\text{sup}}$).

$$\frac{P_{set}}{P_{\text{sup}}} = \frac{2\overline{C}\, h\, A\, g\left(SG-1\right)U_s}{SG\rho_w\, QU_j^{\,2}} = \frac{\pi}{2}\frac{\overline{C}\left(SG-1\right)}{\rho_w\, SG}\frac{Pe}{Fr_j^{\,2}} \tag{1.22}$$

where $Pe$ *and* $Fr_{\text{j}}$ are defined by Equations 1.1 and 1.21, respectively.

Data reported in Table 1.1 make it evident that washout rate, represented by $\overline{C}$, increases as the ratio $P_{set}/P_{\text{sup}}$ of the two powers increases, and Equation 1.22 makes it evident that

the ratio $P_{set}/P_{sup}$ is proportional to the ratio $Pe/Fr_j^2$ . Therefore, the washout rate which is proportional to $\overline{C}$ can be expected to be a function of the ratio $Pe/Fr_j^2$, with the assumption that the ratio $P_{set}/P_{sup}$ is some function of $Pe/Fr_j^2$. To test this hypothesis, the dimensionless variable $\frac{\overline{C}(SG-1)}{\rho_w\, SG}$ was plotted versus $Pe/Fr_j^2$ using the data obtained from all tests in Figure 1.8, which includes all washout data obtained for the 1.8×1.8m, 1.8×0.9m, 1.2×1.2m, 1.2×0.6m, 0.3×0.3m (6×6, 6×3, 4×4, 4×2, and 1×1ft) sumps. It is possible to develop separate charts for geometrically similar sumps, i.e. one for the 1.8×1.8m, 1.2×1.2m, 0.3×0.3m (6×6, 4×4, and 1×1ft), sumps and one for the 1.8×0.9m and 1.2×0.6m (6×3 and 4×2ft) sumps. Equation 23 is the three parameter fitted function that describes the washout rate (effluent concentration) in all standard sumps tested under high flow conditions as a function of $Pe/Fr_j^2$.

$$\frac{C\,(SG-1)}{p_w\, SG} = \frac{8.3\times10^{-6}}{\dfrac{Pe}{Fr_j^{\,2}}} + 4.7\times10^{-4}\; e^{\,-3.18\frac{Pe}{Frj^2}} \qquad (1.23)$$

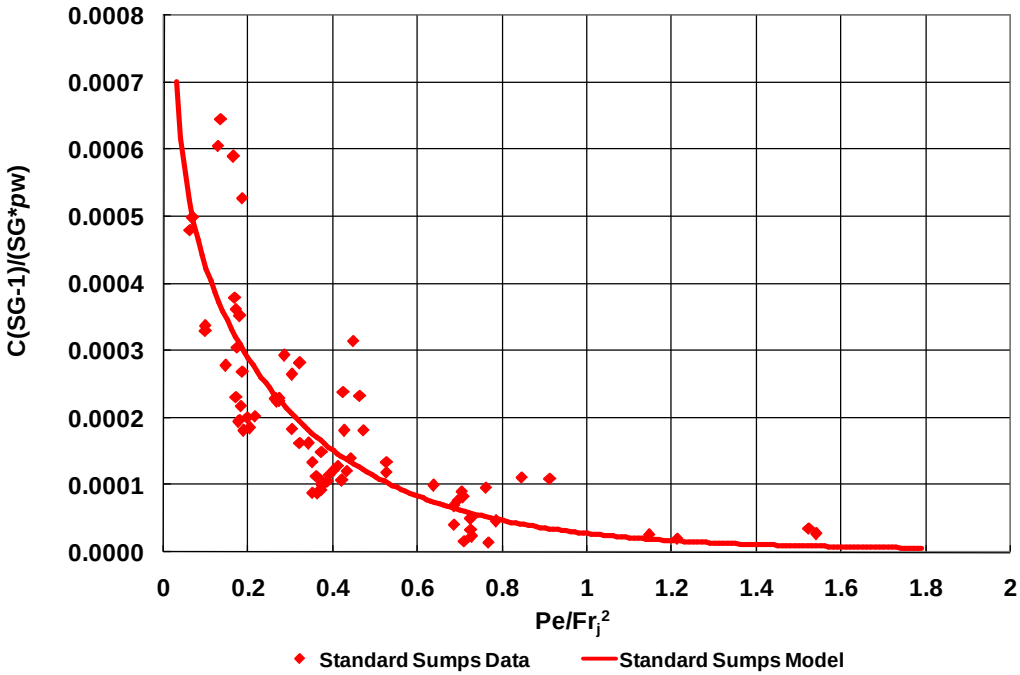


**Figure 1.10: Washout function and experimental data for standard sumps tested.**

It is evident from Figure 1.10 that $Pe/Fr_j^2$ is a suitable dimensionless parameter describing washout in standard sumps, and with a decent accuracy it can be applied to all sizes of standard sumps. At $Pe/Fr_j^2 > 1.5$ entrainment concentrations are very low and at $Pe/Fr_j^2 < 0.2$ they increase rapidly. The dimensionless parameter $Pe/Fr_j^2$ encompasses the effects of particle settling, the sump dimensions, the water inflow discharge and the inflow jet velocity. The Nash-Sutcliffe Coefficient (NSC) of Equation 1.23 and the data is 0.67.

### 1.3.4 Removal Function

Several of the parameters that affect washout (resuspension of suspended sediments) also affect the removal efficiency (settling of suspended sediment) in standard sumps. Since the sump is well mixed, then it is immaterial where the sediment is being supplied into the sump and therefore $Pe/Fr_j^2$ might be effective for describing both the sediment washout and sediment removal efficiency. Utilizing the dimensionless concentration from the washout derivation (Equation 1.24),

$$\hat{C} = \frac{\overline{C}(SG-1)}{\rho_w SG}, \tag{1.24}$$

and recognizing that

$$\eta = \frac{C_{in} - C_{out}}{C_{in}} = \frac{\hat{C}_{in} - \hat{C}_{out}}{\hat{C}_{in}}\ , \tag{1.25}$$

the removal efficiency data obtained in the tests conducted on 1.8×1.8m, 1.8×0.9m, 1.2×1.2m, 1.2×0.6m, and 0.3×0.3m (6×6, 6×3, 4×4, 4×2, and 1×1ft) sumps (some plotted in Figure 1.8 against Péclet number) were re-plotted versus $Pe/Fr_j^2$ (Figure 1.11). In Equation 1.25 $C_{in}$ and $C_{out}$ are the inflow and outflow sediment concentrations respectively. It appears from Figure 1.11 that the parameter $Pe/Fr_j^2$ can be used to explain quantitatively the removal efficiency of standard sumps.

Equation (1.26) is a three-parameter function for the removal efficiency (in %) fitted to data.

$$\eta = 100\,[1 + (0.0275\,Pe/Fr_j^2)^{-1.437}]^{-0.696} \qquad (1.26)$$

The NSC of Equation 1.26 and the data is 0.942 and the Root Mean Square Error (RMSE) for $\eta$ is 8.1%.

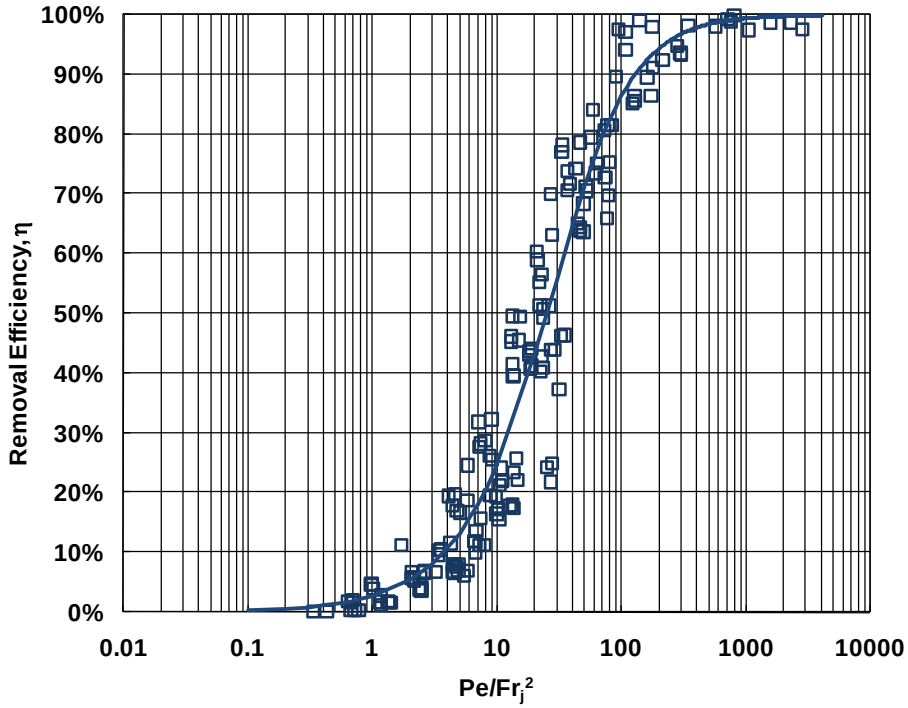


**Figure 1.11: Removal efficiency function for standard sumps tested.**

## 1.4 Uncertainty Analysis

An uncertainty analysis was conducted on both the proposed removal efficiency model and the washout model. Because of the non-normal distribution of the model residuals, it was necessary to use the bootstrap method to determine the uncertainty in the model. Bradley Efron first proposed the bootstrap method in 1979 after working with the jackknife, another re-sampling technique (Lepage 1992). Since then, the bootstrap method has become widely accepted because of its ease of use and the ability to produce accurate results without the knowledge of the data's distribution. This is possible through the production of thousands of new data sets by sampling from the original data. It is

then assumed that these samples represent the entire range of possible values, from which a confidence interval can be developed (Rustomji and Wilkinson, 2008).

The bootstrap method can be applied using three different sampling processes, parametric, non-parametric, and semi-parametric. The non-parametric bootstrap involves sampling from the original values and requires no assumptions regarding the data distribution or the model (Carpenter 2000). Because it is flexible, the non-parametric bootstrap method was used to develop confidence intervals for the proposed models. In the implementation of the bootstrap method, sampling was done without replacement, and the process was repeated between 1000 to 2000 times. In Figures 1.12 and 1.13 the 95% confidence intervals of the removal efficiency and washout functions are plotted. The increased scatter in the washout data has produced wider confidence intervals at high washout rates. However, this process is a reflection of the confidence in the fitted model, i.e. for a 95% confidence interval, 95% of the fitted models will land within these bounds.

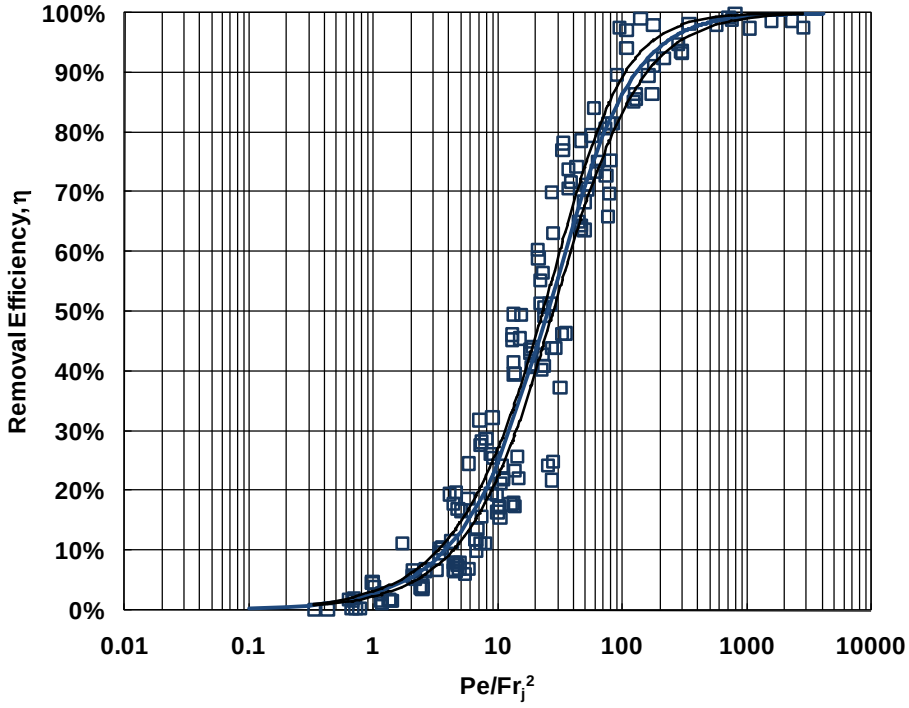


**Figure 1.12: 95% Confidence interval lines for the removal efficiency function of standard sumps tested.**

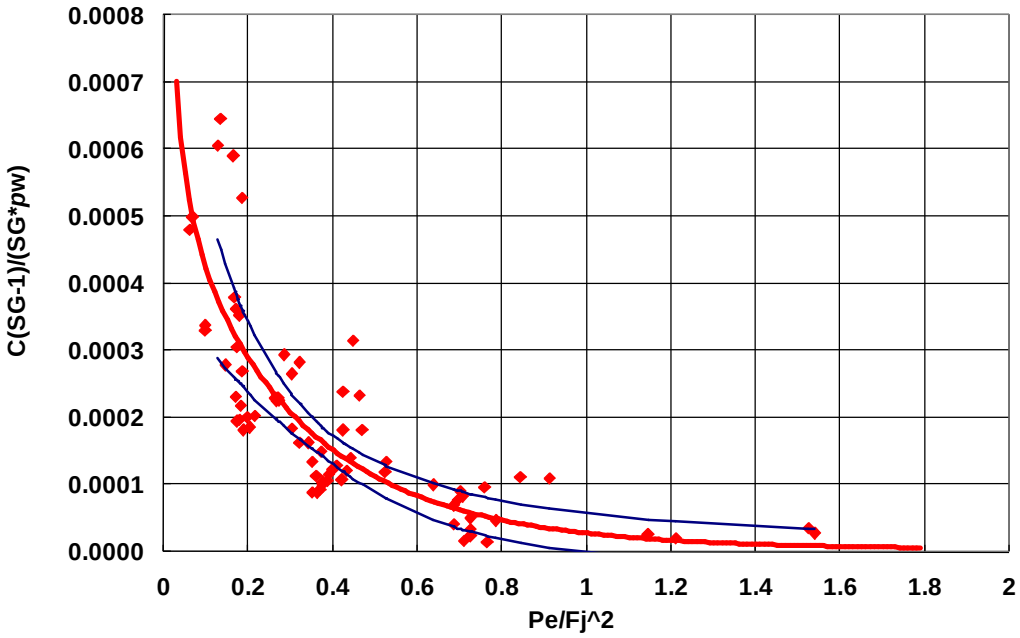


**Figure 1.13: 95% Confidence interval lines for the washout function of standard sumps tested.**

## 1.5 Application of Results

### 1.5.1 Removal Efficiency

Using the plot of removal efficiency versus the dimensionless parameter given in Figure 1.11, it is possible to predict the removal efficiency (i.e. the ability to capture a specific particle size distribution in the influent) of a particular standard sump (of given depth and diameter), on a given day of the year (i.e. water temperature) and for a given storm event (i.e. discharge). It is also possible to determine the main dimensions of a standard sump to meet a particular removal efficiency goal with knowledge of the influent particle size distribution and water discharges.

For example, it may be desired to design a standard sump to remove 20% of a 110μm particle size at a discharge of 17L/s (0.6cfs). A 20% removal efficiency for the standard sump requires a $Pe/Fr_j^2$ value of 7.82. If the water temperature is 7°C (44°F), the settling velocity becomes 0.0045m/s (0.0149ft/s). If the inlet pipe diameter is 38cm (15in) at a

1% slope the inflow velocity will be approximately 0.49m/s (1.6ft/s) for a discharge of 17L/s (0.6cfs). Using Equation 1.26, the only unknowns will be the height and diameter of the sump. For this design, the volume of the sump, $hD^2$, would be 0.71m$^3$ (25ft$^3$). The sump would need to be at least 0.88m (2.9ft) deep and have a 0.88m (2.9ft) diameter to satisfy these requirements.

To complete the sizing of a standard sump requires the development of runoff hydrographs at the outlet of the watershed of interest for an extended period of time. Based on the runoff time series and the potential particle size distribution in stormwater runoff, the annual sediment loading to the sump can be determined. When the annual loading is routed through the removal efficiency function, a minimum length scale can be determined based on a regulatory suspended sediment removal goal.

### 1.5.2 Washout

There are certain constraints and limitations in the application of the washout function. (Equation 1.23). At values of $Pe/Fr_j^2$ greater than 2.3 the washout function is no longer valid. This is the point where the power supplied becomes sufficiently small that no particles can be entrained from the sediment deposit into the water column in the sump. In addition, if the particle size becomes large enough, the suspended sediment concentration in the sump will no longer be well mixed. Thus, the assumptions for the calculation of settling power are no longer valid.

The fitted model presented in Figure 1.10 can be used to predict sediment effluent concentrations from a standard sump for any particle size distribution, particle specific weight, water temperature, sump model (i.e. depth and diameter), sump inlet pipe size, and discharge. Additionally, Equation 1.25 can be used to select standard sump dimensions if a target effluent concentration is limited to a certain value. This process is similar to the one presented above for the removal efficiency function.

For example, the effluent concentration limit may be 200mg/L for the 10 year design storm. If the 10 year design storm peaks at 540L/s (19cfs), and the inlet pipe is 61cm (24in ) in diameter, then the inflow velocity will be approximately 2.04m/s (6.7ft/s ). The

final necessary variables are particle size, water temperature, and specific gravity, which are assumed to be 110μm, 10°C (50°F ), and 2.65 respectively, in this example. Using the input data, the settling velocity becomes 0.0052m/s (0.017ft/s ). We have a goal value of 0.000125 for $C(SG\text{-}1)/(\rho_w SG)$, which produces a $Pe/Fr_j^2$ value of 0.47 from Equation 1.25. The only unknowns are now the sump height and diameter; $hD^2$, is equal to 20.4m$^3$ (722ft$^3$). Thus, the minimum values for the height and diameter of the sump will each be 2.7m (9.0ft ).

In a typical design process, an ultimate long term goal for removal efficiency will be determined. This goal will be a function of both the low flow removal efficiency function and the high flow washout function. Use of these functions entails an iterative process. A sump size would be chosen and tested against a typical rainfall year in the given watershed. If the calculated yearly removal efficiency does not reach the goal, a new sump size would be chosen. The frequency of cleaning will also play an important role in the sizing process. As the sump depth decreases due to sediment capture, increased washout and decreased removal efficiencies will occur.

# Chapter 2. The St. Anthony Falls Laboratory (SAFL) Baffle

The implementation of the 1987 Amendments to the Clean Water Act (Smith 2001) resulted in major changes in the management of stormwater. Detention ponds, infiltration basins, and underground proprietary devices became popular best management practices (BMPs) to meet the National Pollutant Discharge Elimination System (NPDES) regulations in urban areas. Detention ponds and infiltration basins often require large surface areas, i.e. land, which may be expensive or not even available in urban environments. Reaching the stormwater pollution prevention goals can therefore be challenging in urban environments.

Within the last 25 years, many cities, counties and watershed districts have turned to underground stormwater treatment devices to reach their goals. These devices create flow patterns suitable for capturing suspended sediment and floatables. Understanding how well these devices remove particulates from stormwater has been the subject of many studies in the past decade (Carlson et al 2006, Mohseni et al 2007, Wilson et al 2009, Kim et al 2007, Howard et al 2010)

As noted by Saddoris et al. (2010), the overall performance of underground proprietary devices depends on two processes. First, sediment laden water enters the device at low flow rates and the flow conditions in the device help sediment settle to the bottom. This process is often called the device's 'sediment removal efficiency' or 'capture efficiency'. The second process occurs when the previously captured sediment is resuspended and moved from the bottom of the device to the outlet pipe at high water flow rates. This process is called 'washout' (Howard et al., 2010).

Carlson et al. (2006) and Mohseni and Fyten (2007) evaluated two proprietary underground settling devices (hydrodynamic separators) in the laboratory for particulate removal efficiency. A mass balance approach was used starting with the introduction of a known dry quantity of particulates with a known particle size into a measured water flow rate for a set duration and then collecting and measuring the captured sediment quantity following the test. The captured sediment was dried, sieved, and weighed in

order to quantify the removal efficiency of the device. This testing procedure was also implemented in the field by Wilson et al. (2009) on four hydrodynamic separators.

Mohseni and Fyten (2007) also evaluated the washout of sediment from a swirl flow device in the laboratory using a mass balance approach. The measurement of washout required the loading of a known sediment quantity prior to the introduction of water flow rates higher than the maximum design treatment rate specified by the manufacturer. Following the test the amount of sediment remaining in the sump was determined by taking sediment depth measurements throughout the device using a hand held ruler. The volume of sediment and the effluent concentration due to washout could then be determined. Saddoris et al. (2010) also implemented this testing procedure in the field for one device and using load cells in the laboratory for three devices.

The results of these studies indicate that hydrodynamic separators can effectively remove sediment larger than silt from stormwater runoff. The ability of a device to retain this captured sediment is largely dependant on the particular design and the maintenance plan designed by the owner. Some devices may have near zero washout at high flows, while other devices can exhibit sediment effluent concentrations exceeding 1000 mg/L (Saddoris et al. 2010).

Howard et al. (2010) evaluated standard sumps of different sizes for both removal efficiency and washout in the laboratory using the mass balance approach described above. It was found that standard sumps also remove suspended sediment from stormwater runoff but not as well as hydrodynamic separators. However, the main detriment of standard sumps is their propensity for washout. Standard sumps may exhibit washout effluent concentrations up to 1000mg/L. Nevertheless they do have two main advantages over proprietary devices. First, since the standard sump does not require any internal components, it is inexpensive in comparison to hydrodynamic separators. Second, many standard sumps have already been installed in urban stormwater collection systems, at pipe junctures and for maintenance purposes.

Since the standard sump has already been proven effective at capturing sediment, a simple retrofit to increase sediment retention during large storms would be useful. If a simple, effective retrofit could be found to decrease sediment washout from standard sumps, the costs associated with particulate removal could be drastically reduced. In this study the data collected by Howard et al. (2010) on standard sumps were used to design a simple retrofit which can increase the standard sump's ability to retain previously captured sediment at high flow conditions.

## 2.1 Measurement of Flow Pattern in a Sump

To better understand scour and deposition in the sump, Howard et al. (2010) did extensive flow mapping using a 3-dimensional Acoustic Doppler Velocimeter (ADV). Figure 2.1 is a vector plot of the flow pattern in the sump. After entering the sump the flow plunges and creates a downward velocity at the downstream end, an upstream velocity near the sediment bed, and an upward velocity at the upstream end. This circulation pattern, shown in Figure 2.1, can result in scouring of the sediment deposit at the downstream end and more deposition at the upstream end of the sump. It was determined that an effective retrofit should break the circulation pattern and dissipate the energy of the plunging flow.

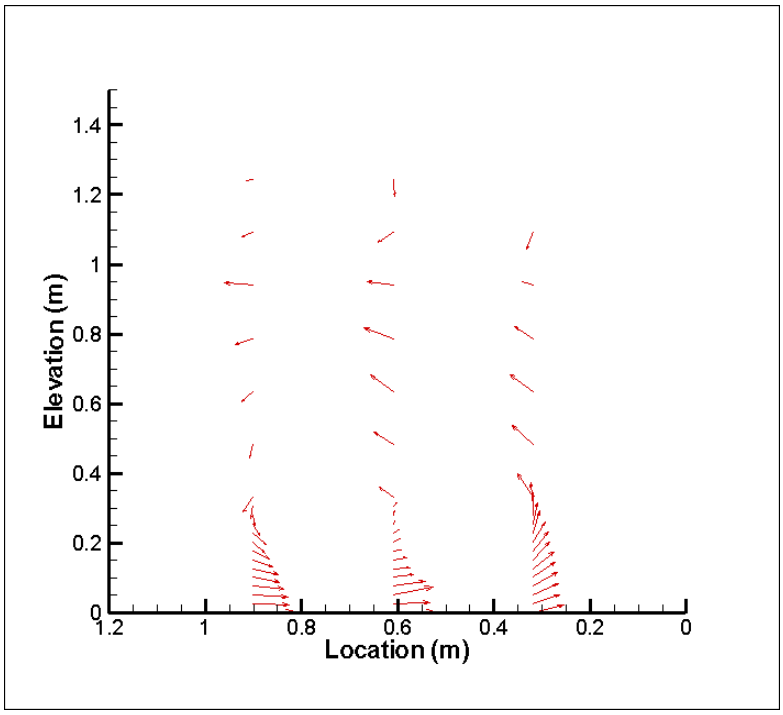


**Figure 2.1: Velocity vectors in a vertical section through the center of a sump. Inflow velocity at elevation 1.2 m (48in) is 0.85m/s (2.8ft/s) from right to left.**

## 2.2 Scale Model Testing of SAFL Baffle Design

Utilizing information on the flow patterns, testing of various sump retrofit designs was initiated in a 1:4.17 Froude scale model. The goal of the retrofit was to reduce the power of the strong circulation pattern. First, a solid baffle was placed perpendicular to the flow in the center of the sump with a space between the bottom of the baffle and the top of the sediment layer. Solid baffles have already been installed in many sumps across the country. The results of the scale model washout tests with two solid baffle designs are given in Figure 2.2.

The bottom of the solid baffles 1 and 2 was located 0.14 and 0.36m (5.5 and 6.8in), respectively, above the top of the sediment layer at the bottom of the sump. The standard sump with a solid baffle had significantly higher washout rates than a sump without the solid baffle. The solid baffle increased washout rates because the same flow rate was required to pass through a smaller cross section between the bottom of the baffle and the

sediment surface. The reduction in cross sectional area increased flow velocities on the sediment surface, which resulted in more sediment entrainment and washout. The solid baffle 1 had more washout than baffle 2 because of the smaller opening between the bottom of the baffle and the sediment surface. To avoid this reduction in cross-sectional area of the flow through the sump, porous baffles were tested. The angle of attack and the porosity were varied in these tests. Figure 2.3 gives the washout results for a variety of porous baffles in the 1:4.17 scale model.

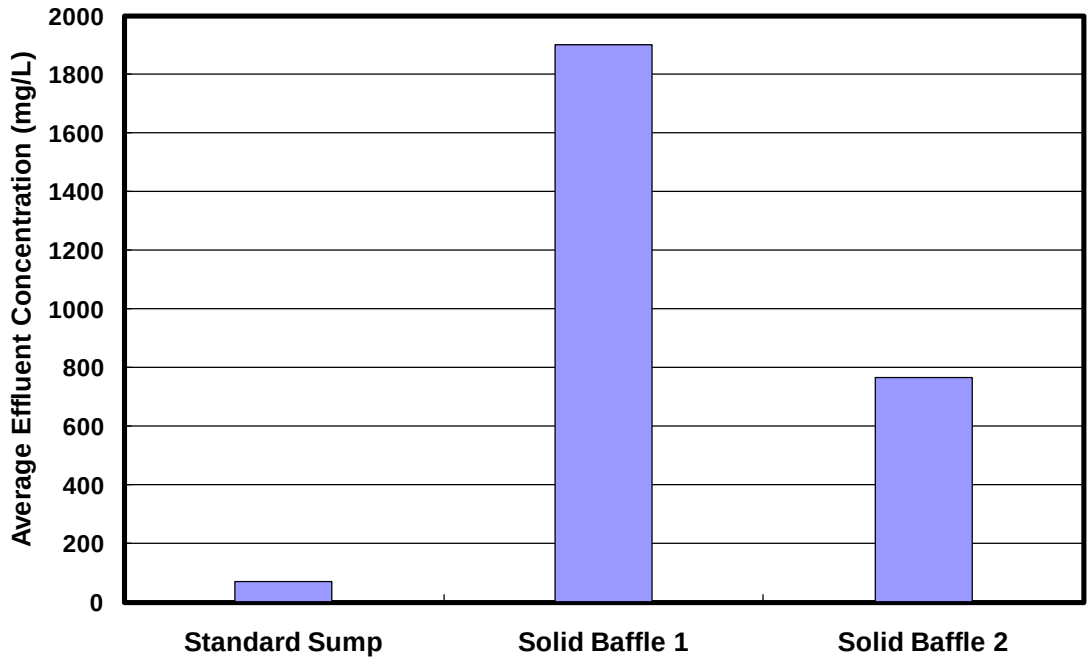


**Figure 2.2: Scale model washout results for two solid baffle designs.**

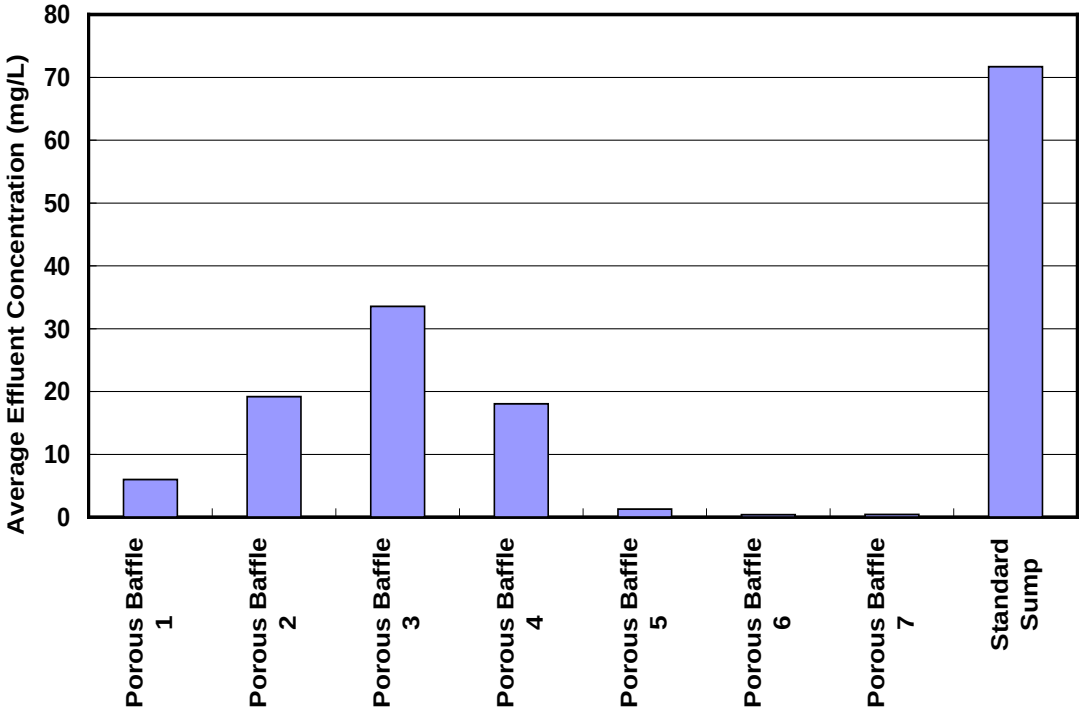


**Figure 2.3: Scale model washout results for several porous baffle designs.**

Baffles 1 and 2 in Figure 2.3 were tested with angles of attack of $+20^{o}$ (striking face pointing down) and $-20^{o}$ (striking face pointing up), respectively, and porosities of 33%. Baffles 3 through 7 were vertical plates with porosities of 33%, 36%, 40%, 46% and 51%, respectively. The flow rate for the tests shown in Figure 2.3 was 5.7L/s (0.2cfs) for the scale model (199L/s or 7cfs in the prototype), and the preloaded sediment was U.S. Silica F-110 (with a median size of 110μm). The duration of all tests shown in Figure 3 was 40 minutes. All porous baffles tested had reduced sediment washout compared to standard sumps. The tests in the scale model showed that with a porosity of 46% to 51% and vertical orientation (baffles 6 and 7), the baffles were very effective: the washout effluent concentration can become negligible. As a reference in Figure 2.3, the standard sump without baffles had effluent concentrations above 70mg/L, almost two orders of magnitude more than standard sumps with porous baffles 6 and 7. For the same flow rate and particle size a baffle with an appropriate orientation and porosity will produce

effluent concentrations near zero. With an appropriate porosity, the baffle will dissipate the energy of the plunging flow by redistributing the flow across the entire sump width.

The improvements to the sump during washout tests were also examined visually. Figure 2.4 is a picture of the standard sump scale model following a washout test without any retrofits; the flow was from left to right in the photo. The sediment scour downstream and the deposition upstream of the sump are clearly evident in the 1:4.17 scale model. Figure 2.5 is a picture of a standard sump with a porous baffle following the washout test; flow was again from left to right. The surface of the sediment deposit remained flat. Porous baffle 6 in Figure 2.3 was determined to be the optimum configuration and was given the name, SAFL Baffle. The SAFL Baffle could now be tested at the full scale for both sediment washout and removal efficiency.

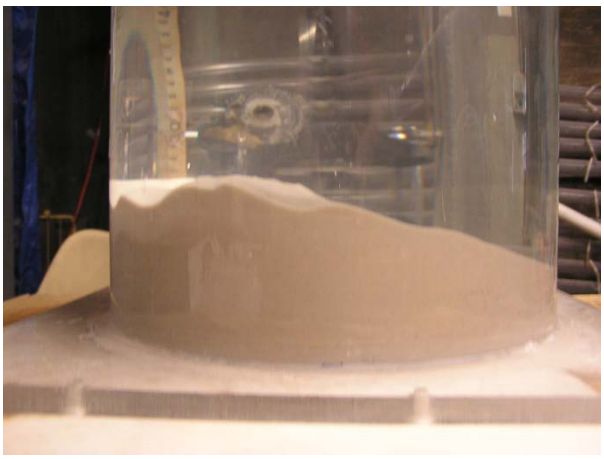

**Figure 2.4: Sediment deposit in the 1:4.17 scale model of a standard sump without any baffles after a washout test at 5.7L/s (0.2cfs).**

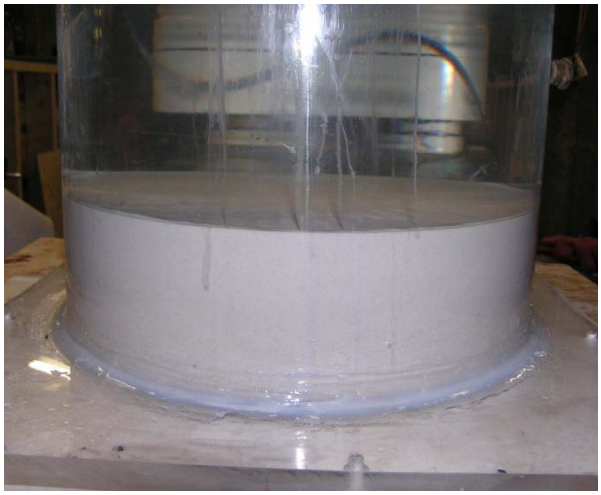

**Figure 2.5: Sediment deposit in the 1:4.17 scale model of a standard sump with baffle no. 7 after a washout test at 5.7L/s (0.2cfs).**

## 2.3 Experimental Setup and Procedure for Full Scale Testing

Two full scale fiberglass sumps were constructed for testing and placed on a test stand in the St. Anthony Falls Laboratory (SAFL) of the University of Minnesota in Minneapolis, Minnesota. The first straight flow-through sump evaluated with the SAFL Baffle was 1.2m (4ft) in diameter and 1.2m (4ft) deep (the height of the inlet pipe from the sump bed), and had 38.1cm (15in) inlet and outlet pipes. There was a one percent drop between the inverts of the inlet and outlet pipes of the sump. The baffle for this setup had circular holes of 2.5cm (1in) diameter and 46% porosity. The frame of the baffle was bolted to the walls of the sump. For good access to the sump bottom during maintenance, the baffle was installed in a vertical position perpendicular to the flow at the center of the sump. Figure 2.6 show an oblique view from above of the inlet pipe and the SAFL Baffle installed in the 1.2m (4ft) sump.

The second straight flow-through sump evaluated with the SAFL Baffle was 1.8m (6ft) in diameter and 0.9m (3ft) deep with 0.61cm (24in) inlet and outlet pipes. This baffle had 7.7cm (3in) holes and 46% porosity. The baffle installation in the 1.8m (6ft) sump was similar to the 1.2m (4ft) sump. Each sump was connected to the SAFL plumbing system which provides approximately 13.7m (45ft) of head of Mississippi River water. The free surface flow into each sump through the 0.31m (12in) supply pipe was measured using

two Pitot cylinders (Silberman 1947). The free surface flow into both sump configurations was controlled using a hydraulic gate valve in the supply pipe.

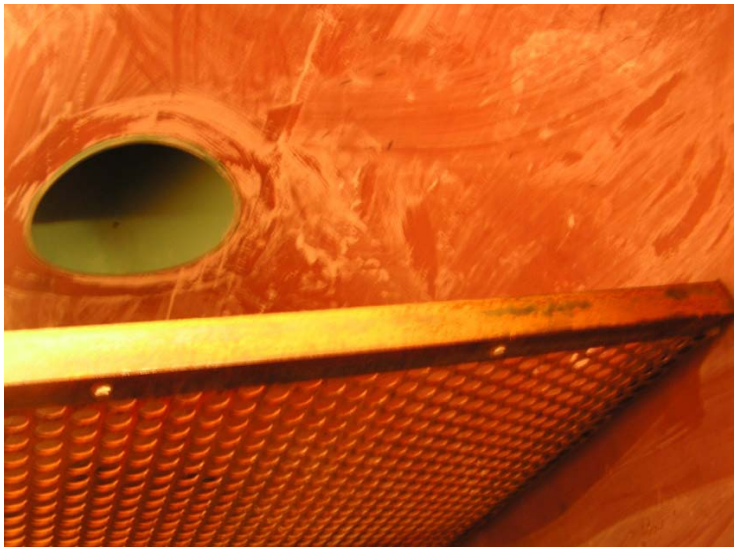

**Figure 2.6: SAFL Baffle in the 1.2x1.2m (4ft × 4ft) sump.**

For removal efficiency testing, sediment was fed at a calibrated rate as a slurry from a Schenk AccuRate sediment feeder into the inlet pipe approximately one foot upstream of the sump. For washout testing, the sump, mounted on precision strain gauge load cells, was weighed before, during and after tests for accurate determination of the sediment loss during the test (Saddoris et al., 2010).

For the 1.2m (4ft) sump removal efficiency testing, washout rates were measured at flow rates of 17.0, 34.0, 51.1 and 64.1L/s (0.6, 1.2, 1.8, and 2.4cfs) in triplicate. The 1.8m (6ft) sump was tested at flow rates of 51.1, 99.3 and 150.4, and 198.2L/s (1.8, 3.5, 5.3, and 7cfs). Additional removal efficiency tests were conducted at flow rates of 8.5, 11.3 and 14.2 L/s (0.3, 0.4, and 0.5cfs) to obtain removal efficiencies of approximately 100%.

Carlson et al. (2006) showed that the results of removal efficiency tests are independent of the influent concentration when sediment particles could not impact each other's flow path. Therefore, the influent concentrations of the removal efficiency tests were varied between relatively low values between 100 to 200mg/L. According to Wilson et al.

(2009), a total sediment input of 10 to 20kg minimized the errors associated with sediment collection at the bottom of the sump. The duration of each test was selected a priory so that 10 to 20kg of sediment would be fed for each test. The test duration was one hour for the lowest flow and 18 minutes for the higher flow rates. Three distinct particle sizes were used for the tests. The median sediment sizes were 545μm (500μm to 589μm), 303μm (250μm to 355μm), and 107μm (88μm to 125μm).

Washout tests required preloading of the sump with sediment and then applying high flow rates to the sump. Prior to each washout test, 0.31m (12in) of U.S. Silica sand F-110 with a median particle size of 110μm was placed in the sump. Great care was taken to ensure that the initial conditions were identical for all tests.

Two methods were used to measure the weight of sediment in the sump before and after each test. In the first method, stick measurements were taken to measure the depth of wet sediment at 24 locations, which were then used to estimate an average depth of the wet sediment. The difference between the average depths of sediment before and after each test was used to determine the volume of the washed out sediment. Tests were conducted on several sediment samples to determine the bulk specific weight under water. It typically varied from 1650kg/$m^3$ to 1730kg/$m^3$ (spec. gravity from 1.65 to 1.73) for the 8 to 10 samples taken from different locations and depths within the sump.

In the second method, precision strain gauge load cells were used to weigh the sediment deposited in the sump before and after each test. The 5,000 lb precision strain gauge load cells from Tovey Engineering, Inc. provided accurate measurements of weight throughout each test. In order to take accurate weight measurements it was necessary to record both the initial and final weight measurements with the same elevation of water in the sump. A water elevation difference of 1mm between the initial and the final weighing would produce an error of about 2.7kg (6lbs). Therefore, the water level in the sump was measured before and after each test using a precision manometer. The flow rate in the washout tests on the 1.2m and 1.8m (4ft and 6ft) sumps varied from 78 to 156L/s (2.75 to

5.5cfs) and 142 to 539L/s (5 to 19cfs), respectively. The flow rate in each test was kept constant.

## 2.4 Results of Full Scale Testing

The effects of the SAFL Baffle on the washout rate and removal efficiency of standard sumps were investigated in 1.2×1.2m (4×4ft) and 1.83×0.91m (6×3ft) sumps (The first number is the sump diameter and the second number is the height of the sump below the outlet pipe invert). The results are presented and compared with those obtained in standard sumps with no baffle.

### 2.4.1 Removal Efficiency Results

Removal efficiencies measured in the 1.2×1.2m (4×4ft) sump are plotted against water flow rate in Figure 2.7. With the SAFL Baffle installed, there is a significant increase in removal efficiency (approximately 15%) of small size particles (110μm) at low flow rates, e.g. below 14.2L/s (0.5cfs). The SAFL Baffle could not improve the performance for large particles at 14.2L/s (0.5cfs) and below, because the sump without the SAFL baffle is already achieving near 100% removal. At medium flow rates, around 28.4L/s (1cfs), however, standard sumps with the SAFL Baffle exhibited between 10 to 20% increase in removal efficiency for all particle sizes tested. At higher flow rates, above 42.6L/s (1.5cfs), smaller sediment particles were not removed more efficiently with the SAFL Baffle in place, but larger sediment sizes were removed approximately 10% more efficiently.

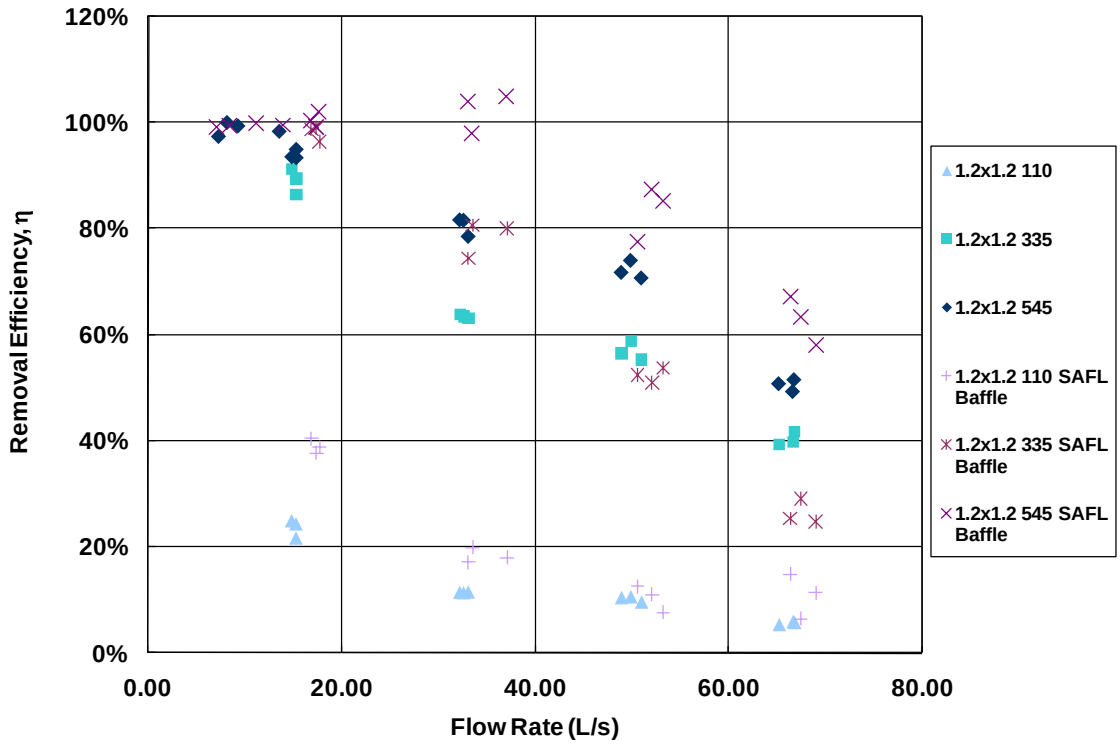


**Figure 2.7: Sediment removal efficiencies in the 1.2×1.2m (4×4ft) sump with and without the SAFL Baffle. Legend gives sump size (diameter x depth in m), and particle size in μm.**

The results of the removal efficiency tests conducted in the 1.8×0.9m (6×3ft) sump are shown in Figure 2.8. At very high and very low flow rates the removal efficiencies were more or less the same for all particle sizes tested. However, at median flow rates and median particle sizes, the sump exhibited a 15% (on average) increase in sediment capture with the SAFL Baffle.

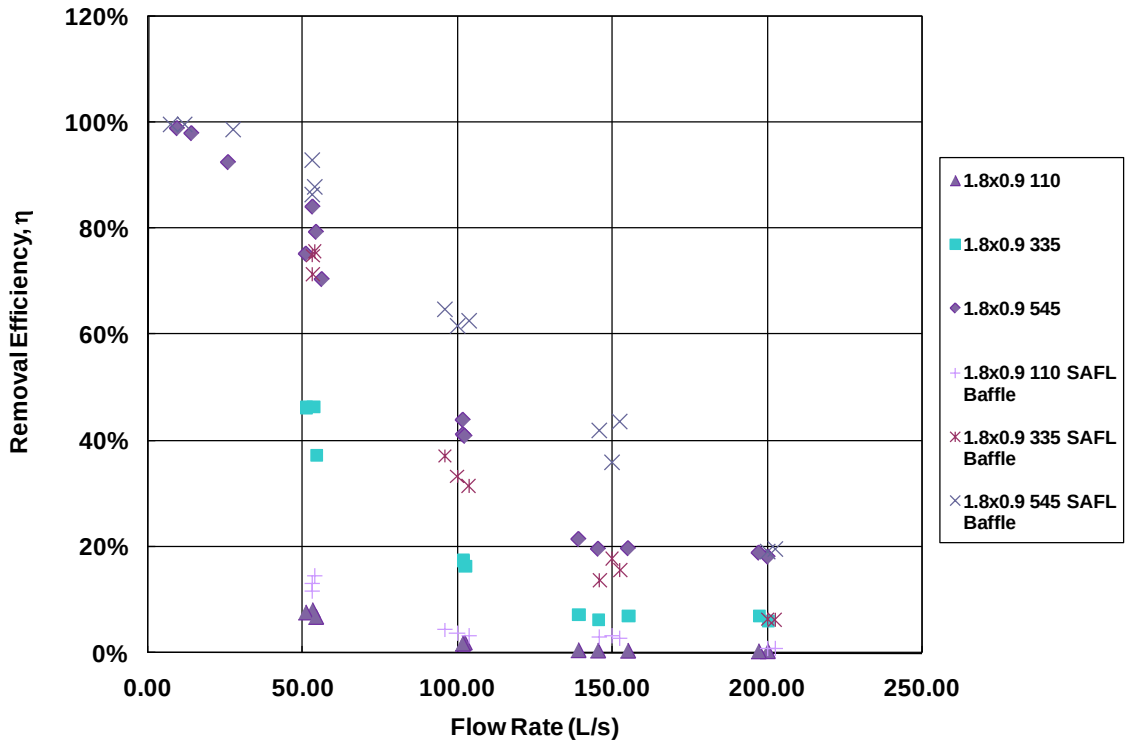


**Figure 2.8: Sediment removal efficiencies in the 1.8×0.9m (6×3ft) sump with and without the SAFL Baffle. Legend gives sump size (diameter x depth in m), and particle size in μm.**

### 2.4.2 Washout Results

Figure 2.9 gives the results of the washout tests both with and without the SAFL Baffle. In Figure 2.9 the sediment concentration in the sump effluent is plotted against the flow rate through the sump. As can be seen, the baffle reduced effluent concentrations from 500mg/l to nearly 0mg/l at 142L/s (5cfs) flow. Several tests gave negative washout values, i.e. the weight of the system had increased by the end of the washout test. Since such an increase was physically impossible, the results had to be attributed to the uncertainty of the load cells. The maximum uncertainty of the load cells used in the tests was +/- 10 lbs and in the majority of tests conducted with the SAFL Baffle the measured washout was less than 10 lbs after two hours of testing. To obtain results outside the uncertainty range of the load cells, it was decided to use a finer sediment which would be expected to give a higher washout rate. The top three inches of the F110 Silica sand (median size = 110μm) in the sump were therefore replaced with SCS250 (median size =

45µm), and the tests were repeated. The results obtained with the SCS250 were similar to those obtained with the F110 silica sand, i.e. effluent concentrations obtained with the SCS250 stayed near zero after the sump was subjected to high flow rates for two hours (Figure 9).

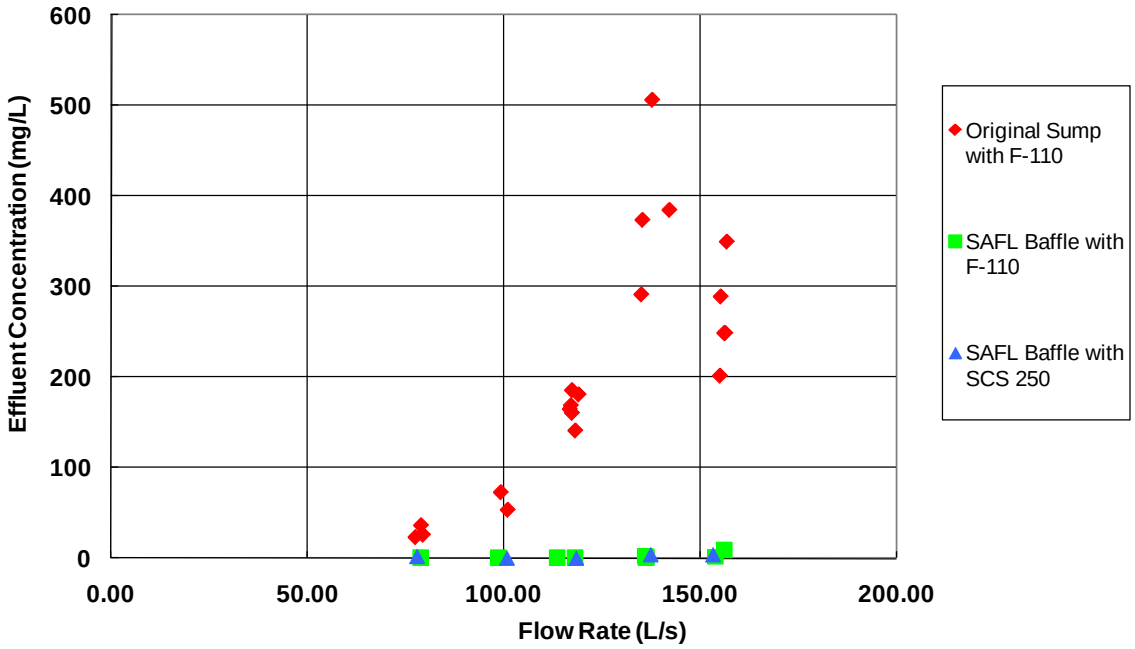


**Figure 2.9: Effluent concentrations of the washout tests in the 1.2×1.2m (4×4ft) sump with and without SAFL Baffle.**

The tests conducted on the 1.2m (4ft) deep sump with the SAFL Baffle were very encouraging. It was therefore decided to test the SAFL Baffle in a shallow sump of 1.8m (6ft) diameter which imposes more challenging conditions for washout, i.e. increased the flow rates and decreased sump depth. The baffle used in this test series had the same porosity, but had 7.6cm (3in) holes, compared to the 2.5cm (1in) holes used in the 1.2m (4ft) sump tests with the SAFL Baffle. In practice, 7.6cm (3in) holes allow more trash to pass through the sump reducing the clogging potential of the baffle. A SAFL Baffle with 7.6cm (3in) holes might be more desirable and require less maintenance. Figure 2.10 provides a comparison of the results of the tests conducted on the 1.8× 0.9m (6×3ft) sump with and without the SAFL Baffle. The baffle greatly improved the ability of the

sump to retain sediment. At 454L/s (16cfs) flow, the SAFL Baffle decreased the sediment washout concentration from 800mg/L to 50mg/L.

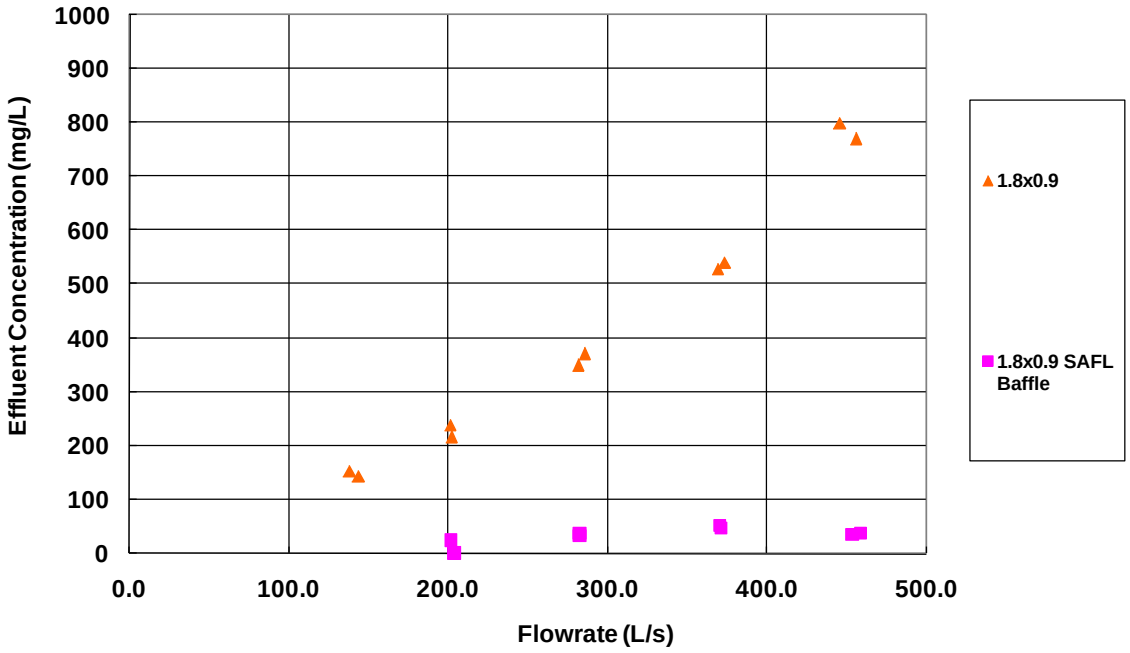


**Figure 2.10: Effluent concentrations of the washout tests in the 1.8×0.9m (6×3ft) sump with and without SAFL Baffle.**

.

A review of the removal efficiency and washout test data shows that with the SAFL Baffle retrofit, even small particle sizes which have collected in the sump will remain in the sump at high flow conditions. For instance, a 1.2×1.2m (4×4ft) sump can capture 107µm particles during a flow event with a magnitude of 28L/s (0.6cfs). Even though only 18% of this sediment may be captured in antecedent storm runoff events, all of what is captured will remain in the sump even when a 156L/s (5.5cfs) flow passes through the sump. Without the SAFL Baffle, most of this sediment may be washed out of the sump during the large storm event.

### 2.4.4 Head Loss Induced by the SAFL Baffle

A possible concern with the SAFL Baffle is the increase in head loss. If the head loss is too high at high flow rates, the sump may overtop and/or cause flooding upstream of the sump. With the baffle in the sump, the maximum increase in the head loss was determined to be 0.061m (0.2ft) at a flow rate of 51L/s (5.5cfs). This increase in head loss does not cause a problem for most storm sewer designs. Figure 2.10 is a plot of head loss vs. flow rate with and without the SAFL Baffle in place.

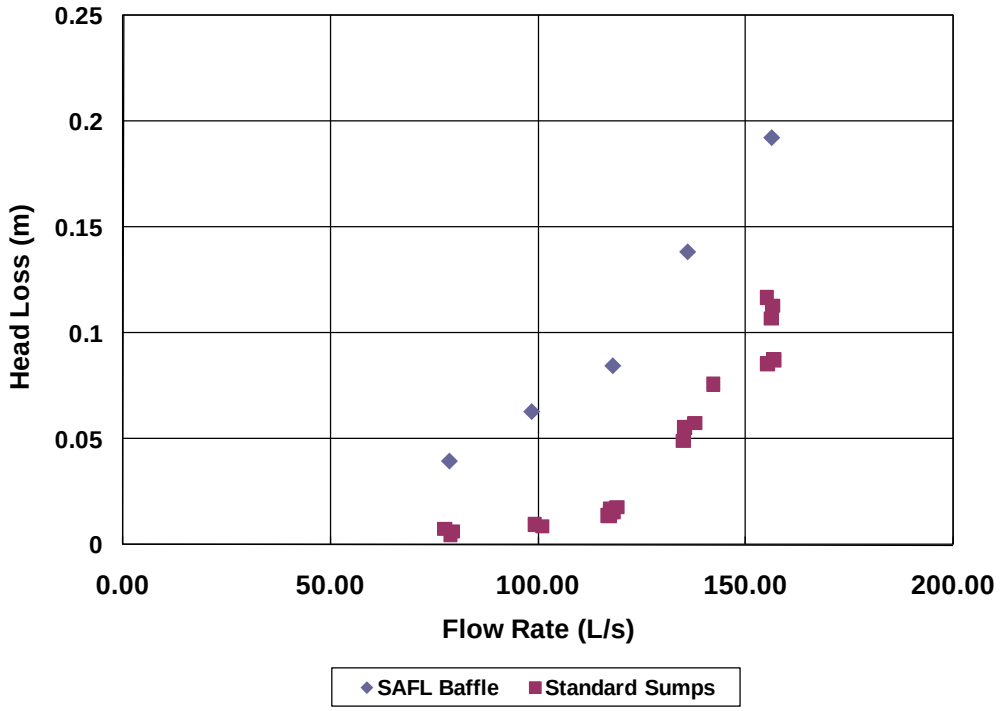


**Figure 2.11: Head loss vs. flow rate in a 1.2×1.2m (4×4ft) sump with and without the SAFL Baffle.**

### 2.4.3 Interpretation of the Results

Standard sumps in storm sewer systems are designed and built with a variety of sump diameters and depths, and inlet and outlet pipe diameters. They also have to handle a wide range of flow rates, water temperatures, sediment sizes and densities. Since standard sumps can not be tested for all possible combinations, it is necessary to find parameters and a function which can effectively scale the test results.

The Péclet number, given in Equation 2.1, has been used by Carlson et al. (2006), Mohseni et al. (2007) and Wilson et al. (2009) to scale removal efficiency in underground settling devices.

$$Pe = \frac{Us * h * D}{Q} \tag{2.1}$$

In Equation 2.1, $U_s$ is the settling velocity calculated according to Cheng (1997), $h$ is the sump depth, $D$ is the sump diameter, and $Q$ is the flow rate. As shown by Wilson et al. (2009), when removal efficiency is plotted versus the Péclet number, a performance function in the form of removal efficiency vs. Péclet number can be developed for a stormwater treatment device. The Péclet number works well to describe the performance of a single device under a wide range of flow rates, particle sizes and densities, and water temperatures. However, by changing the length scales in Equation 2.1, the function may not be capable of predicting the removal efficiency for all sizes, i.e. a different fitted model may be required for each device size.

Howard et al. (2010) measured removal efficiencies and washout rates in five different standard sumps: 1.8×1.8m (6×6ft), 1.8×0.9m (6×3ft), 1.2×1.2m (4×4ft), 1.2×0.6m (4×2ft) and 0.3×0.3m (1×1ft). Howard et al. (2010) were able to derive washout and removal efficiency functions of standard sumps for this wide range of length scales using the ratio of the Péclet number to the square of the inflow jet Froude number ($Pe/Fr_j^2$) as the scaling parameter. The inflow jet Froude number was defined as $Fr_j^2=U_j^2/(gD)$. In the derivation, the power supplied by the inflow was compared to the power required for the incipient motion of the particles, entrainment into the water column and lifting to the height of outflow pipe. The Péclet-Froude number ratio was obtained from the ratio of the settling power of particles to the power supplied. Since the same parameters also affect the removal efficiency of standard sumps, the removal efficiency was re-plotted versus the Péclet-Froude number ratio and it was shown that $Pe/Fr_j^2$ can predict particle capture under low flow conditions.

For washout, a three parameter, nonlinear, decreasing function was fitted to the data to develop a washout function. The fitted sump washout function is given in Equation 2.2.

$$\frac{C(SG-1)}{\rho_w SG} = \frac{x}{Pe/Fr_j^{\,2}} + ye^{-tPe/Fr_j^{\,2}} \tag{2.2}$$

In Equation 2.2, *x*, *y* and *t* are fitted parameters, *C* is the effluent concentration, *SG* is the particle specific gravity and $\rho_w$ is the density of water.

For removal efficiency, a three parameter, nonlinear, increasing function was fitted to the data to create a removal efficiency function. The function is described by the relationship shown in Equation 2.3.

$$\eta = \left[\frac{1}{R^b} + \frac{1}{\left(a\ Pe/Fr_j^{\,2}\right)^b}\right]^{-1/b} \tag{2.3}$$

In Equation 2.3, *R*, *a*, and *b* are fitted parameters and $\eta$ is predicted removal efficiency.

### 2.4.5 Increase of Removal Efficiency by the SAFL Baffle

Figure 2.12 is a plot of the measured removal efficiency versus the dimensionless parameter $Pe/Fr_j^2$. The data plotted have been obtained in tests conducted on the 1.2×1.2 m (4×4ft) and 1.8×0.9m (6×3ft) sumps with and without the SAFL Baffle in place. The fitted function for removal efficiency $\eta$ (in %) in the 1.2×1.2m (4×4ft) and 1.8×0.9m (6×3ft) standard sumps is given by Equation 2.4.

$$\eta = 100\ [1 + (0.026\ Pe/Fr_j^2)^{-\,1.473}]^{-0.679} \tag{2.4}$$

Equation 2.4 has a Root Mean Square Error (RMSE) of 8.2%. The RMSE was calculated as described by Wilson et al. (2009). The fitted function for the 1.2×1.2m (4×4ft) and 1.8×0.9m (6×3ft) standard sump with the SAFL Baffle is given by Equation 2.5.

$$\eta = 100\ [1 + (0.0208\ Pe/Fr_j^2)^{-\,2.1216}]^{-0.4713} \tag{2.5}$$

Equation 2.5 has an RMSE of 4.9%.

Using the fitted functions (Equations 2.4 and 2.5), it is possible to predict the removal efficiency for a particular standard sump, influent particle size, water temperature, and

flow rate, both with and without the SAFL Baffle. A standard sump can also be designed to meet a particular removal efficiency goal for a given influent particle size and flow rate.

The results presented in Figure 2.12 suggest that standard sumps retrofitted with the SAFL Baffle exhibit only a slight increase in removal efficiency at $Pe/Fr_j^2$ values above approximately 50. Overall, with the SAFL Baffle in place, there will be no large benefit for the removal of suspended sediments from stormwater runoff.

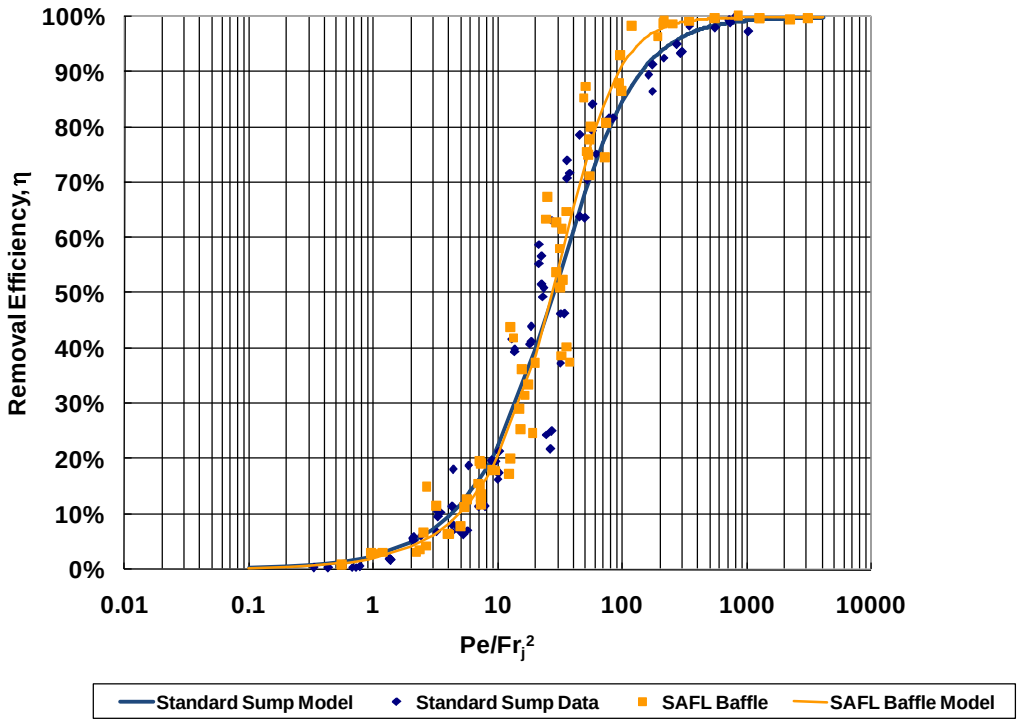


**Figure 2.12: Comparison of removal efficiency for standard sumps with and without SAFL Baffle.**

It is important to note that at a given flow rate and for a given particle size and density, the value of $Pe/Fr_j^2$ is not the same for standard sumps with and without the SAFL Baffle. The inflow jet velocity is an important parameter in $Pe/Fr_j^2$ and it is squared in the denominator. Any slight increase in head loss due to the presence of the SAFL Baffle causes a decrease in the jet velocity and therefore a larger increase in $Pe/Fr_j^2$. Figure 2.13

is a plot of estimated $Fr_j^2$–values in the experiments versus flow rate. The figure gives the data for standard sumps with and without the SAFL Baffle.

For the same flow rate, the standard sump with a SAFL Baffle has lower $Fr_j^2$-values.Thus, for the same flow rate, a sump with the SAFL Baffle will have a higher $Pe/Fr_j^2$, i.e. for the same flow rate and particle size, a sump with the SAFL Baffle will be more efficient in removing suspended sediments as was already shown in Figures 2.7 and 2.8.

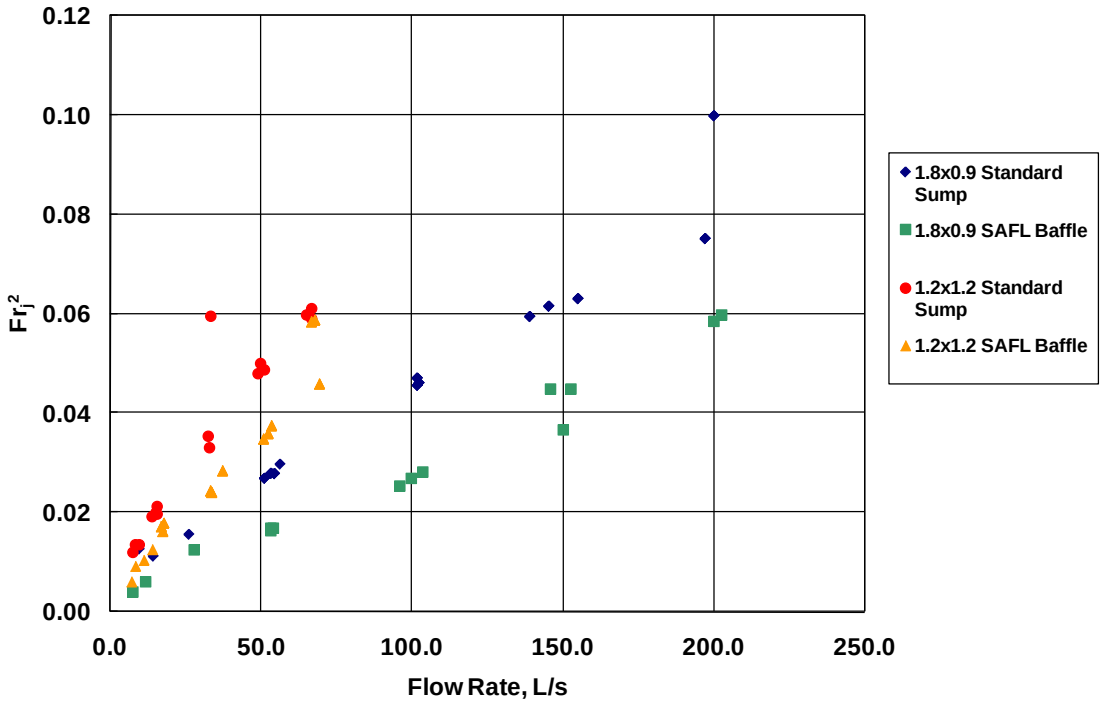


**Figure 2.13: Comparison of the inflow $Fr_j^2$ in sumps with and without the SAFL Baffle for a variety of flow rates. Legend gives sump size (diameter x depth in ft).**

As an example of the use of the $Pe/Fr_j^2$ functions consider that it may be desired to design a standard sump that removes 20% of the suspended sediment with a 110μm particle size at a flow rate of 17L/s (0.6cfs). If the inflow pipe has a diameter of 0.38m (15 inches), the typical inflow jet velocity will be about 0.49m/s (1.6ft/s). A 20% removal efficiency for the standard sump occurs at a $Pe/Fr_j^2$ value of 8.22. If the water temperature is $35^o$ F, the settling velocity will be 0.45cm/s (0.0129ft/s). At 17L/s (0.6cfs),

the value of $hD^2$ will become 2.8 $m^2$ (30.4$ft^2$). The sump would need to be at least 0.94m (3.1ft) deep and 0.94m (3.1ft) in diameter to satisfy these requirements.

For complete sizing, continuous hydrologic modeling of the drainage basin is required (Mohseni et al. 2009; NCHRP 2006). By incorporating the removal efficiency function into a hydrologic model, the annual sediment removal and removal efficiency can be determined for a known particle size distribution. Through trial and error minimum length scales can be determined based on a total suspended sediment removal goal.

### 2.4.6 Reduction in Washout by the SAFL Baffle

Figure 2.14 gives the results of washout tests for the standard sump with and without the SAFL Baffle. The washout functions of the standard sumps with and without the SAFL Baffle are provided in Equations 2.6 and 2.7, respectively.

$$\frac{C(SG-1)}{p_w SG} = \frac{1.42\times10^{-6}}{\frac{Pe}{Fj^2}} + 4.11\times10^{-7}\, e^{-0.689\frac{Pe}{Fj^2}} \tag{2.6}$$

$$\frac{C(SG-1)}{p_w SG} = \frac{8.3\times10^{-6}}{\frac{Pe}{Fj^2}} + 4.7\times10^{-4}\, e^{-3.18\frac{Pe}{Fj^2}} \tag{2.7}$$

The Nash-Sutcliffe Coefficient (NSC) for Equation 2.6 is 0.62 and the NSC value for Equation 2.7 is 0.67. The NSC was calculated as described by Wilson et al. (2009).

These two fitted models can be used to predict sediment effluent concentrations from a standard sump for any combination of particle size, particle specific weight, water temperature, sump depth, sump diameter, sump inlet pipe size, and flow rate. In addition, the models can also be used to select the required design of a standard sump if a desired effluent concentration at high flow rate has been selected. The selection process is similar to the one when the removal efficiency is given.

Equation 2.6 (the washout function for the sump retrofitted with the SAFL Baffle) is a non-linear function of $Pe/Fr_j^2$. It is evident that this function holds true for $Pe/Fr_j^2$ values smaller than 1.3, i.e. when the removal efficiency reaches about 3% (Figure 2.12).

Referring to Equation 2.6, the estimated effluent concentration is limited to 54mg/L for very small particles and very high flow rates. This value is slightly larger than the maximum measured effluent concentration of 50mg/L in the laboratory experiments discussed earlier. The discrepancy between 50mg/L and 54mg/L is small in the context of washout concentrations observed in hydrodynamic separators, and can be ignored at this time.

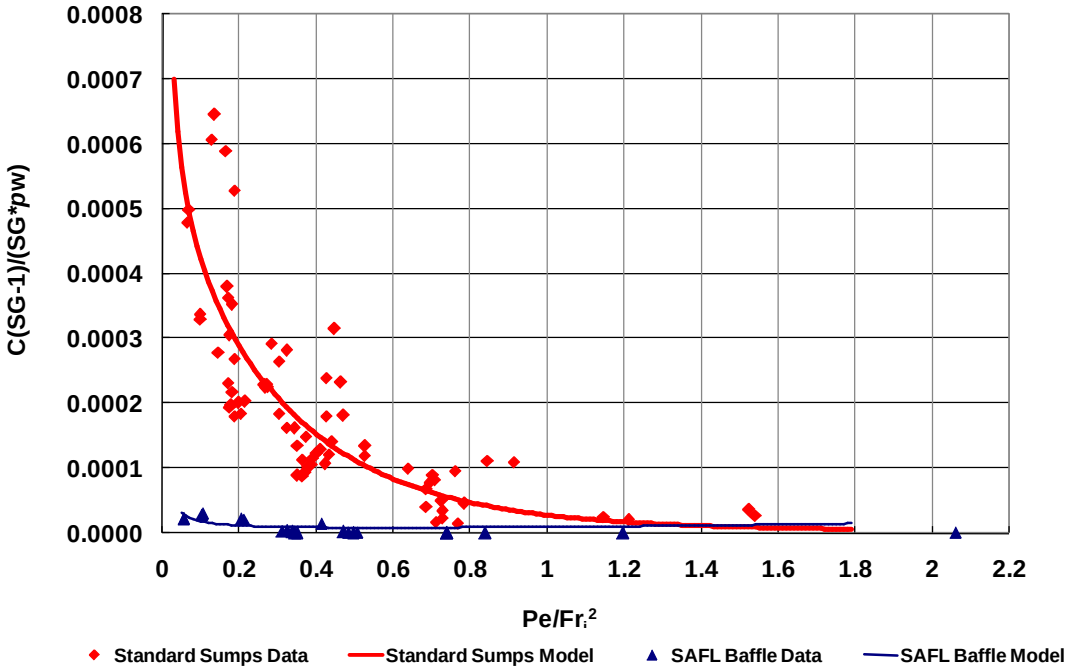


**Figure 2.14: Comparison of washout functions of standard sumps with and without the SAFL Baffle.**

When a sump without the SAFL Baffle is designed for high sediment removal efficiency and low washout, the controlling process will be washout. This is due to the high propensity of standard sumps for washout. In other words, to meet the washout requirements a larger sump size may be required than to achieve the required removal efficiency. The opposite is true if the sump is designed with the SAFL Baffle. The baffle creates a high reduction in washout, and the size of the sump will be determined by the required removal efficiency.

## Summary and Conclusions

In this study the ability of a standard sump in a storm sewer system to remove (capture, entrap, settle) suspended particles larger than silt under low to moderate flow conditions has been evaluated. Also evaluated has been the ability to release (scour, washout) previously captured particles from a standard sump under high flows. The tests were conducted on five different sump configurations. The diameter to depth ratios of the five configurations were 1.2m×1.2m (4ft×4ft), 1.2m×0.6m (4ft×2ft), 1.8m×1.8m (6ft×6ft), 1.8m×0.9m (6ft×3ft), and 0.3m×0.3m (1ft×1ft).

The removal efficiency tests typically consisted of 40 data points collected during 15 tests. The sediment sizes tested were divided into three narrow distributions: 89-125μm, 251-355μm, and 500-589μm. The maximum flow rate tested was 68L/s (2.4cfs) for the 1.2m (4ft) sumps and 198L/s (7.0cfs) for the 1.8m (6ft) sumps.

The washout tests consisted of 15 to 20 data points, each representing an individual test for one particle size (110μm). The maximum tested flow rate, selected based on the 10-year design storm, was 156L/s (5.5cfs) for the 1.2m (4ft) sump and 538L/s (19.0cfs) for the 1.8m (6ft) sump.

The results of the study provide insight into the processes that influence sediment capture and washout in standard sumps. The testing has proven that the standard sump is effective at collecting (removing) sediment at flow conditions below the 1 year design storm. The major shortcoming of the standard sump is its inability to retain the captured sediment under high flows. This is especially evident in tests of shallow sumps. Reducing sump depth increases the potential for sediment washout.

During the washout tests it was noted that sediment deposited at the bottom of the sump was moved upstream and deposited by a large vortex in the lower portion of the sump. At the end of a washout experiment the sediment surface would have a strong slope from a

high elevation just below the inlet pipe to a low elevation below the outlet pipe. The vortex flow pattern was studied using an Acoustic Doppler Velocimeter. The results document the rotation induced by downstream flow at the water surface, and the associated flow in upstream direction along the sediment bed. The circulation pattern is what allows the previously captured sediment to be removed from the sump, decreasing the effectiveness of the sump as a sediment capturing device. Thus, frequent maintenance is necessary for the standard sump to be considered an effective stormwater settling device.

Performance functions for predicting removal efficiency and washout potential in standard sumps have been derived, using a new dimensionless number, $Pe/F_j^2$ as the scaling parameter. This dimensionless number can be used to accurately predict the removal efficiency or effluent concentration or for a particular flow rate, sump diameter and depth, inlet pipe diameter, water temperature, and sediment size. Uncertainty analyses for both removal efficiency and sediment washout were conducted using the bootstrap method. The uncertainty analyses resulted in pointwise confidence intervals which can be used to evaluate the effectiveness of the proposed models for removal efficiency and washout potential.

Standard sumps are effective in removing sediment at low flow conditions. The major downfall of standard sumps is their inability to retain the captured sediment under high flow conditions. This is even more pronounced in shallow sumps. Either frequent maintenance or a retrofit should be designed for the standard sump to be considered an effective stormwater settling device.

One such retrofit, a simple porous baffle called SAFL Baffle, was designed to break the circulation pattern and dissipate the energy of the plunging inflow to a sump. The SAFL Baffle with 46% porosity and a vertical orientation was first evaluated in a 1:4.17 Froude scale model. After the baffle was evaluated in the scale model, it was installed in the 1.2×1.2m (4×4ft) and 1.8×0.9m (6×3ft) sumps for prototype testing. The results of the full scale tests showed that the SAFL Baffle will improve sediment capture by 10 to 15%

and decrease effluent concentrations from 800mg/L to a maximum of 50mg/L for sediment washout. Removal efficiency and washout functions were developed from the measured values using the dimensionless parameter $Pe/Fr_j^2$, i.e. the ratio of Péclet number to the square of the inflow jet Froude number. The performance functions can be used for the prediction of yearly removal efficiencies for sumps retrofitted with the SAFL Baffle and aid in the design of new sumps including a SAFL Baffle.

# References


Akiyama, J. and H.G. Stefan (1985). Gradually Varied Turbidity Current With Erosion and Deposition. *Journal of Hydraulic Engineering* 111(12):1473-1496.

American Society of Civil Engineers (1975). *Sedimentation Engineering.* ASCE Manuals and Reports on Engineering Practice-No. 54, Washington D.C.

Avila, H., and R. Pitt (2008). Evaluating Scour Potential in Stormwater Catchbasin Sumps Using a Full-Scale Physical Model and CFD Modeling. *Proceedings of the Water Environment Federation*, WEFTEC. pp. 6958-6977.

Butler, D., and S. H. P. G. Karunaratne (1995). The Suspended Solids Trap Efficiency of the Roadside Gully Pot. *Water Research* 29(2): 719-729.

Carlson, L., O. Mohseni, H.G. Stefan, and M. Lueker (2006). Performance Evaluation of the BaySaver Stormwater Separation System. St. Anthony Falls Laboratory, University of Minnesota, *Project Report* No. 472, University of Minnesota, Minneapolis, MN

Carpenter, J. and J. Bithell (2000). Bootstrap Confidence Intervals: when, which, what? A practical Guide for Medical Statisticians." *Statistics in Medicine* 19: 1141-164.

Cheng, N (1997). A Simplified Settling Velocity Formula for Sediment Particle. *Journal of Hydraulic Engineering* 123(2). 149-152.

DeGroot, G. P., J.S. Gulliver, and O. Mohseni (2009). Accurate Sampling of Suspended Solids. *Proceedings World Environmental and Water Resources Congress*, pp. 807-813.

Dhamotharan, D., J.S. Gulliver and H.G. Stefan (1981). Unsteady one-dimensional settling of suspended sediment. *Water Resources Research*, 17(4):1125-1132.

Faram, M.G., and R. Harwood (2003). A Method for the Numerical Assessment of Sediment Interceptors". *Water Science and Technology* 47(4): 167-174.

Howard, A.K., O. Mohseni, J.S. Gulliver, and H.G. Stefan (2010). Assessment and Recommendations for Operation of Standard Sumps as Best Management Practices for Stormwater Treatment. St. Anthony Falls Laboratory, University of Minnesota, *Project Report*, June 2010, University of Minnesota, Minneapolis, MN

Kang, J.H., P.T. Weiss, C.B. Wilson and J.S. Gulliver (2008). Maintenance of Stormwater BMPs: Frequency, Effort and Cost. *Stormwater* 9(8): 18-28.

Kim, J, S. Pathapati, B. Liu and J. Sansalone. (2007) "Treatment and Maintenance of Stormwater Hydrodynamic Separators: A Case Study". Proceedings of the 9th Biennial Conference on Stormwater Research and Watershed Management.

Lepage, R. and L. Billard (1992). *Exploring the Limits of Bootstrap*. Wiley Inc. New York, New York.

Mohseni, O., and A. Fyten (2007). Performance Assessment of Modified ecoStorm Hydrodynamic Separator. St. Anthony Falls Laboratory Univ. of Minnesota. *Project Report* No. 495B, University of Minnesota, Minneapolis, MN.

Mohseni, O, Kieffer, J. M., and Koehler, J. A. (2009). A Tool for the Performance Assessment of Hydrodynamic Separators. Proceedings of World Environmental and Water Resources Congress in Kansas City, Missouri, American Society of Civil Engineers, Reston Va.

National Cooperative Highway Research Program (NCHRP). (2006). "Evaluation of Best Management Practices for Highway Runoff Control". Report #565. pp. 89-96.

Pitt, R. (1985). Characterizing and Controlling Urban Runoff Through Street and Sewerage Cleaning. *USEPA Water Engineering Research Laboratory Report*, Cincinnati, Ohio.

Rustomji, P. and S.N. Wilkinson (2008). Applying Bootstrap Resampling to Quantify Uncertainty in Fluvial Suspended Sediment Loads Estimated Using Rating Curves. *Water Resources Research* 44: 1-12.

Saddoris, D.A., K. D. McIntire, O. Mohseni, and J. S. Gulliver (2010). Hydrodynamic Sediment Retention Testing. *Mn/DOT Research Services Report* No. 2010-10. 2010

Schetz, J. A. (1993). Boundary Layer Analysis. Prentice Hall, Englewood, New Jersey. pp. 388.

Silberman, E. (1947). The Pitot Cylinder. St. Anthony Falls Hydraulic Laboratory, University of Minnesota. *Circular* No. 2. 1947

Smith, E. (2001). Pollutant Concentrations of Stormwater and Captured Sediment in Flood Control Sumps Draining an Urban Watershed. *Water Research* 35: 3117-126.

Wilson, M. A., J.S. Gulliver, O. Mohseni, and R.M. Hozalski (2007). Performance Assessment of Underground Stormwater Devices. St. Anthony Falls Laboratory, University of Minnesota *Project Report* No. 494.

Wilson, M. A., O. Mohseni, J.S. Gulliver, R.M. Hozalski, and H.G. Stefan (2009). Assessment of Hydrodynamic Separators for Stormwater Treatment. *Journal of Hydraulic Engineering* 135(5): May 1.